



Statens vegvesen

Ferry free E39 –Fjord crossings Bjørnafjorden

304624

Rev.	Publish date	Description	Made by	Checked by	Project appro.	Client appro.
0	15.08.19	Issued for use	TNNgu	EivBj	KH	
Client		 Statens vegvesen				
Contractor		Contract no.:				
 		18/91094				

Document name:

K12 – Ship impact, Bridge girder

Document no.:

SBJ-33-C5-OON-22-RE-015-B

Rev.:

0

Pages:

50



CONCEPT DEVELOPMENT FLOATING BRIDGE E39 BJØRNAFJORDEN

K12 – Ship impact, Bridge girder

Norconsult 

 DR. TECHN.
OLAV OLSEN

 Prodtex
Production / Technology / Excellence

 IFE
Pure Logic
The science of production resourcing

HEYERDAHL ARKITEKTER AS

 H&BB

 MIKO
MARINE AS

 BUKSÉR og
BERGING

 FORCE
TECHNOLOGY

 SWERIM

REPORT

Project name:

CONCEPT DEVELOPMENT FLOATING BRIDGE E39
BJØRNAFJORDEN

Document name:

K12 – SHIP IMPACT, BRIDGE GIRDER

Project number: 5187772/12777
Document number: SBJ-33-C5-OON-22-RE-015-B

Date: 15.08.2019
Revision: 0
Number of pages: 50

Prepared by: Thanh Ngan Nguyen
Controlled by: Eivind Bjørhei
Approved by: Kolbjørn Høyland

Summary

General

The case of a ship impact on the K12 – end-anchored floating bridge with mooring system over Bjørnafjorden, is studied. The report seeks to clarify how the structure responds to ship impact locally on the bridge girder by explicit nonlinear finite element analysis.

Deckhouse-girder collision is studied for the girder at three impact heights on the deckhouse: At deck 2, inclined at deck 4 and between deck 2 and 3. In the local collision analyses, the bridge girder is fixed against movements at the boundaries of the modelled girder.

Impact energies to be dissipated at different parts of the bridge are defined in the Design Basis [1]. The impact energies are based on risk analysis performed by Rambøll and considers annual probability of return and Heinrich factor among others.

Input from local collision response to global collision assessment is the force-displacement curves. The force-displacement curve gives the relationship between the contact force and the indentation between ship deckhouse and bridge girder. These curves are put into the global finite element model of the bridge structure by a non-linear connector element representing the ship and bridge girder locally.

When global assessment has been conducted, several response parameters are revealed for further local damage evaluation. This includes as the most important the amount of energy that is dissipated locally and the indentation between ship deckhouse and bridge girder.

The impact energies defined in the Design Basis are too high to presuppose only local dissipation, and external dynamics must be accounted for. Reference is made to the global assessment report [2]. Results for local impact response are given for chosen parameters as basis for comparison.

Deckhouse-girder collision characteristics

In the local simulations performed, the deckhouse dissipates most of the energy while the girder is less damaged. The distribution of energy dissipation between the deckhouse and the girder is in the area 85/15 [%]. This distribution causes the compression of the bridge girder to stabilize at approximately 0.8 m. The displacement of the connector element obtained from the global assessment is therefore close to the indentation in the deckhouse alone.

Figure 1 shows the force-displacement curves for the different locations investigated. Table 1 evaluates the maximum and mean contact force for the period up to 8 m ship displacement from these curves.

> *Table 1 Maximum and mean contact force [MN] impact deckhouse-girder 0-8 m ship displacement*

Location	Max. contact force [MN] 0-8 m	Mean contact force [MN] 0-8 m
At deck 2	44	30
Inclined at deck 4	38	27
Between deck 2 and 3	35	20

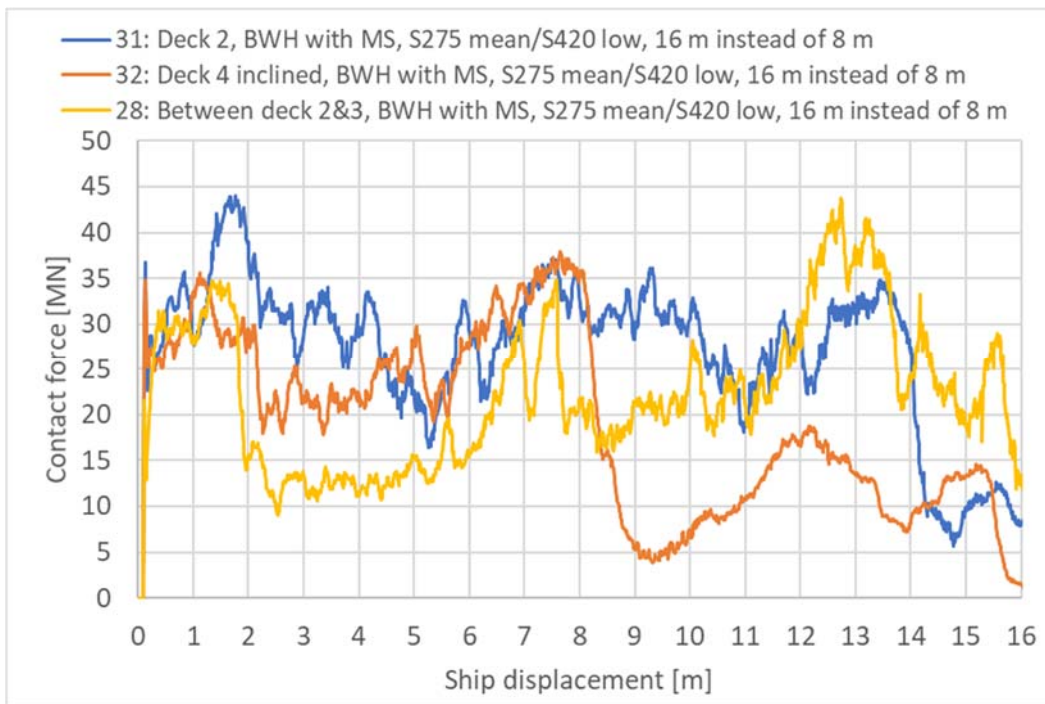


> Figure 1 Contact force [MN] impact deckhouse-girder

Sensitivity of ship impact response

The ship impact simulations performed are sensitive to several parameters. In addition to location of impact, sensitivity is studied for material parameters, material damage models, element type, mass scaling and reinforced bridge girder.

The simulation of deckhouse-girder collision is less sensitive to change in material parameters of the bridge girder and sensitive to change in material parameters of the deckhouse. The reason is because the deckhouse is the weaker structure in collision with the bridge girder.

Residual capacity of bridge girder

Residual capacity of the bridge girder is evaluated with push-over analyses of the intact and damaged bridge girder with either pure moment about strong axis or pure moment about weak axis. Stresses and deformations from the ship impact analysis are preserved for the residual evaluation. The residual capacities shown in Table 2 is the apex of the resulting load-rotation curves. A simple evaluation of the section forces shows that the damaged bridge girder has enough capacity for the 100-year environmental loading.

> Table 2 Residual capacity of bridge girder after ship impact

	Moment about strong axis	Moment about weak axis
Intact bridge girder	100 %	100 %
4 m ship displacement	92.3 %	99.6 %
8 m ship displacement	88.2 %	99.6 %
12 m ship displacement	87.4 %	97.4 %
16 m ship displacement	84.7 %	96.0 %

Table of Content

1	INTRODUCTION	8
1.1	Current report	8
1.2	Project context	8
1.3	Project team	8
1.4	Project scope	9
2	INTRODUCTION TO SIMULATIONS	11
2.1	General	11
1.1	Design philosophy.....	11
3	MATERIAL MODELLING	13
3.1	General	13
3.2	Yield surface and plastic work hardening.....	13
3.3	Fracture and necking instability	13
3.4	Verification	15
4	SIMULATION MODELS	19
4.1	Geometry	19
4.2	Materials	21
4.3	Mesh and element formulations	23
4.4	Analysis setup	25
5	SIMULATIONS	28
5.1	Load cases.....	28
5.2	Response parameters.....	29
5.3	Response.....	29
6	INPUT TO GLOBAL COLLISION ASSESSMENT	43
7	SUMMARY AND CONCLUSIONS	44
7.1	Compilation of response	44
7.2	Discussion	45
7.3	Further work	48
8	REFERENCES	49

APPENDIX A – Abaqus terminology
APPENDIX B – Mesh and material sensitivity study
APPENDIX C – Sensitivity of ship impact response

1 INTRODUCTION

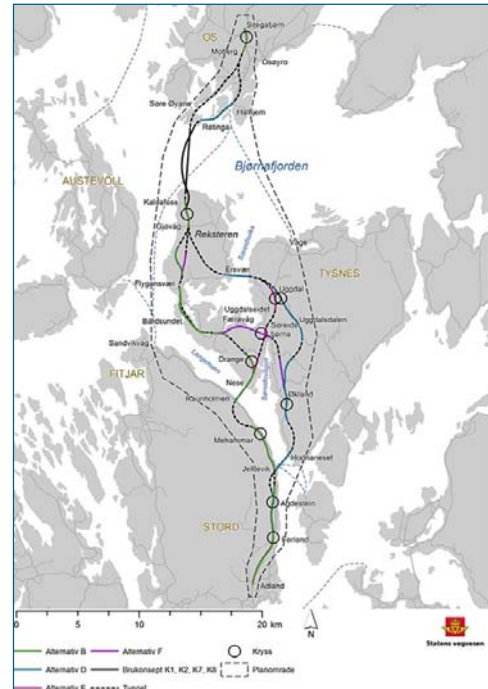
1.1 Current report

This report seeks to clarify how the K12 – end-anchored floating bridge with mooring system over Bjørnafjorden, responds to ship impact locally for the bridge girder.

1.2 Project context

Statens vegvesen (SVV) has been commissioned by the Norwegian Ministry of Transport and Communications to develop plans for a ferry free coastal highway E39 between Kristiansand and Trondheim. The 1100 km long coastal corridor comprise today 8 ferry connections, most of them wide and deep fjord crossings that will require massive investments and longer spanning structures than previously installed in Norway. Based on the choice of concept evaluation (KVU) E39 Aksdal Bergen, the Ministry of Transport and Communications has decided that E39 shall cross Bjørnafjorden between Reksteren and Os.

SVV is finalizing the work on a governmental regional plan with consequence assessment for E39 Stord-Os. This plan recommends a route from Stord to Os, including crossing solution for Bjørnafjorden, and shall be approved by the ministry of Local Government and Modernisation. In this fifth phase of the concept development, only floating bridge alternatives remain under consideration.



1.3 Project team

Norconsult AS and Dr.techn.Olav Olsen AS have a joint work collaboration for execution of this project. Norconsult is the largest multidiscipline consultant in Norway, and is a leading player within engineering for transportation and communication. Dr.techn.Olav Olsen is an independent structural engineering and marine technology consultant firm, who has a specialty in design of large floating structures. The team has been strengthened with selected subcontractors who are all highly qualified within their respective areas of expertise:

- Prodtex AS is a consultancy company specializing in the development of modern production and design processes. Prodtex sits on a highly qualified staff who have experience from design and operation of automated factories, where robots are used to handle materials and to carry out welding processes.
- Pure Logic AS is a consultancy firm specializing in cost- and uncertainty analyses for prediction of design effects to optimize large-scale constructs, ensuring optimal feedback for a multidisciplinary project team.
- Institute for Energy Technology (IFE) is an independent nonprofit foundation with 600 employees dedicated to research on energy technologies. IFE has been working on high-performance computing software based on the Finite-Element-Method for the industry, wind, wind loads and aero-elasticity for more than 40 years.
- Buksér og Berging AS (BB) provides turn-key solutions, quality vessels and maritime personnel for the marine operations market. BB is currently operating 30 vessels for

harbour assistance, project work and offshore support from headquarter at Lysaker, Norway.

- Miko Marine AS is a Norwegian registered company, established in 1996. The company specializes in products and services for oil pollution prevention and in-water repair of ship and floating rigs, and is further offering marine operation services for transport, handling and installation of heavy construction elements in the marine environment.
- Heyerdahl Arkitekter AS has in the last 20 years been providing architect services to major national infrastructural projects, both for roads and rails. The company shares has been sold to Norconsult, and the companies will be merged by 2020.
- Haug og Blom-Bakke AS is a structural engineering consultancy firm, who has extensive experience in bridge design.
- FORCE Technology AS is engineering company supplying assistance within many fields, and has in this project phase provided services within corrosion protection by use of coating technology and inspection/maintenance/monitoring.
- Swerim is a newly founded Metals and Mining research institute. It originates from Swerea-KIMAB and Swerea-MEFOS and the metals research institute IM founded in 1921. Core competences are within Manufacturing of and with metals, including application technologies for infrastructure, vehicles / transport, and the manufacturing industry.

In order to strengthen our expertise further on risk and uncertainties management in execution of large construction projects Kåre Dybwad has been seconded to the team as a consultant.

1.4 Project scope

The objective of the current project phase is to develop 4 nominated floating bridge concepts, document all 4 concepts sufficiently for ranking, and recommend the best suited alternative. The characteristics of the 4 concepts are as follows:

- K11: End-anchored floating bridge. In previous phase named K7.
- K12: End-anchored floating bridge with mooring system for increase robustness and redundancy.
- K13: Straight side-anchored bridge with expansion joint. In previous phase named K8.
- K14: Side-anchored bridge without expansion joint.

In order to make the correct recommendation all available documentation from previous phases have been thoroughly examined. Design and construction premises as well as selection criteria have been carefully considered and discussed with the Client. This form basis for the documentation of work performed and the conclusions presented. Key tasks are:

- Global analyses including sensitivity studies and validation of results
- Prediction of aerodynamic loads
- Prediction of hydrodynamic loads
- Ship impact analyses, investigation of local and global effects
- Fatigue analyses
- Design of structural elements
- Marine geotechnical evaluations
- Steel fabrication
- Bridge assembly and installation

- Architectural design
- Risk assessment

2.1 General

The case of a ship impact on the K12 – end-anchored floating bridge with mooring system over Bjørnafjorden, is studied. Distribution of impact energies are given in the Design Basis [1].

This report seeks to clarify how the structure responds to ship impact locally for the bridge girder.

1.1 Design philosophy

Ship impacts are defined as accidental load conditions related to a recurrence period of 10 000 years. The Norwegian Public Roads Administration (NPR) has in handbook N400 [3] set this as the limit where less likely events are disregarded.

In the Accidental Limit State (ALS) all loads are applied with partial load factors of 1.0, and structures may be designed utilizing lower material safety factors than in Ultimate Limit State (ULS) and Serviceability Limit State (SLS). Local collapse is acceptable, provided the global stability can be maintained to prevent total collapse. For the bridge girder, this means that the bridge girder can be damaged causing a reduced stiffness, as long as the bridge can sustain a post-impact phase according to NS-EN 1991-1-7 [4].

Impact loads depend on the relationship between the incoming ships mass and velocity (total impact energy) and the system response. The system response is depending on the mass (m), the combined stiffness (k) of the structure and ship, and the system damping (c). Simplified it can be described with the equation of motion below, where the impact load F varies over time.

$$m\ddot{x} + c\dot{x} + kx = F(t)$$

The dynamic response from the impact energy depend on ship stiffness and stiffness and mass of the structure. To ensure a ductile design the analysis considers the differences in stiffness. This is done by transferring the energy through the following steps:

1. Ship bow-pontoon/deckhouse-girder impact. Represented by a force-displacement curve, based on local analysis.
2. Bridge structure. Represented by global finite element model.

By combining the stiffness and mass in different parts of the system in one model, we obtain a realistic energy distribution. For the connection between ship and bridge girder this can be illustrated with the graph in Figure 2-1. The graph shows that the mobilized resistance is equal in the two systems, and that this balance, together with the force-displacement relations, give the corresponding deformations and energy absorption in each part of the system.

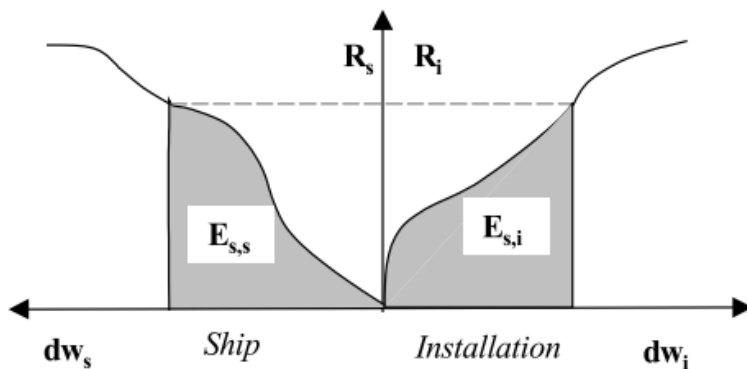


> Figure 2-1 Force equilibrium based on force-displacement curves (from [5])

Figure 2-2 shows an overview of the workflow used for the ship impact analysis, here presented by the screening analysis of girder impacts.

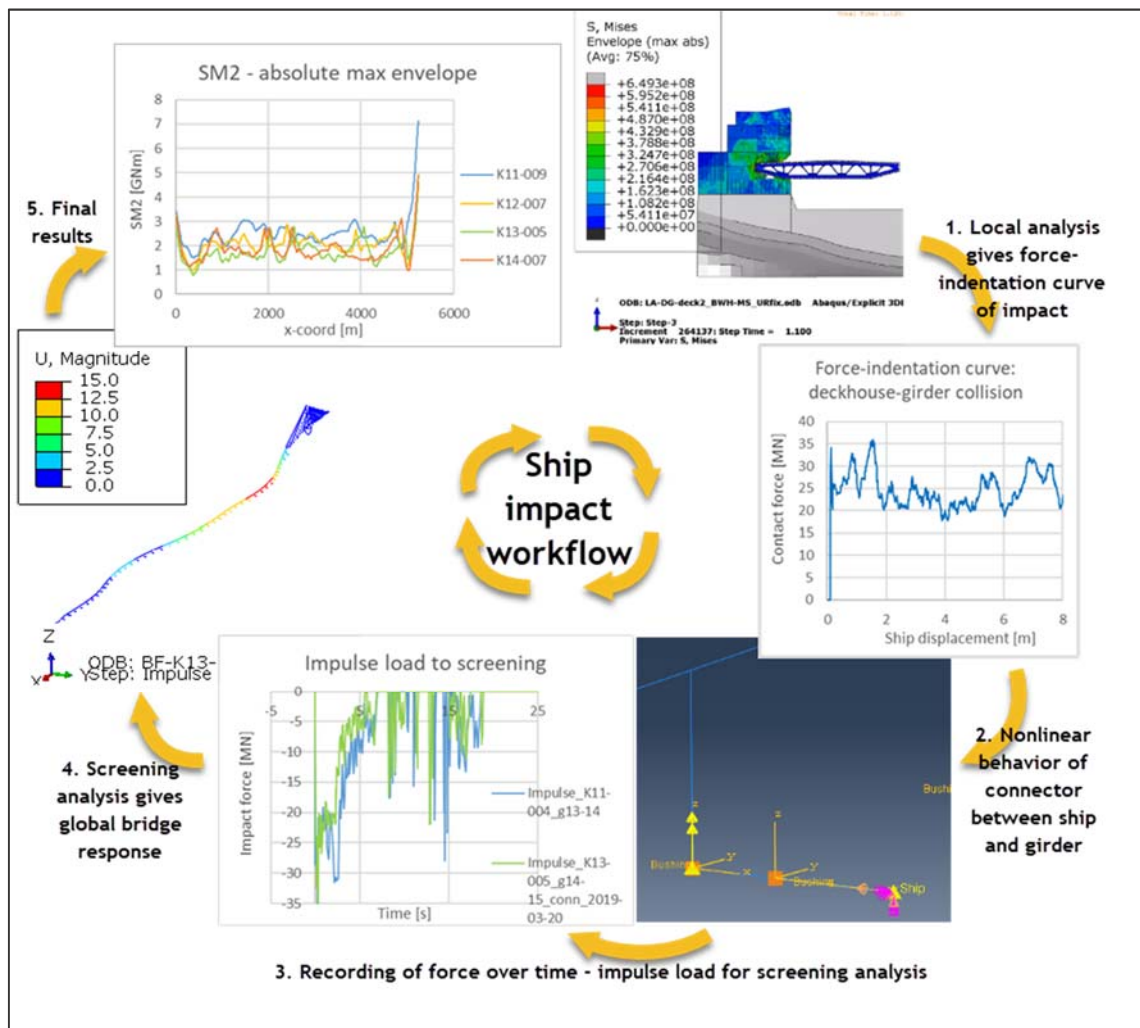


> Figure 2-2 Ship impact workflow. Local analysis: step 1. Global analysis and post-processing step 2-5.

3 MATERIAL MODELLING

3.1 General

A well-defined and robust material model is essential in the simulations of local response for the ship impact scenarios. Robustness of the material model in this context imply e.g. that the material model is not sensitive to small changes in simulation set-up. Due the nature of the concept development, the actual material properties are not known.

To obtain a representative response for the design materials it is chosen to use parameters according to DNVGL-RP 208 [6], DNVGL-OS-B101 [7], isotropic hardening and the Bressan-Williams-Hill (BWH) instability criteria.

3.2 Yield surface and plastic work hardening

Material description in the elastic range is applied using the standard material module in Abaqus [8].

Properties defining the material in the plastic range and damage evolution is defined through a subroutine developed at NTNU. The subroutine is provided by the Client and is described in Kevin Ofstads master thesis [9], and further description of the material model is given in [10]. For simplicity this material model is in this report referred to as the BWH model.

The von Mises yield surface is used for the isotropic materials. The yield surface defines when plastic strains are generated.

Isotropic hardening is applied to define how the yield surface changes for plastic strain. The isotropic hardening is considered a suitable model for problems with large plastic straining and where the strain does not continuously reverse direction sharply [8]. The rate-independent plasticity model uses associated flow. The hardening rule is given as:

$$\sigma_{eq} = Kp^n$$

where K is the power law modulus, p is the plastic strain and n is the power law exponent.

It is chosen not to include strain-rate dependence in the material. The effect of strain-rate hardening can according to [11] be significant, but the effect is less on complex structures than on uniaxial test.

3.3 Fracture and necking instability

In recent work performed at NTNU [9] [12] [13] [14] and in phase 3 of the Bjørnafjorden project [15] two main damage evolution models have been used in ship impact analysis, i.e. the Bressan-Williams-Hill (BWH) instability criterium and the Rice-Tracy-Cockcroft-Latham (RTCL) criterium. In the current work it is chosen to use the BWH criterium due to computation time, availability and compatibility with the Abaqus software. The material model is described in short, for details it is referred to [9] and [10] For verification of the received model, simulations have also been performed with both strain- and stress-based material models in Abaqus, see Appendix B [16] for results.

The BWH model combine Hill's criterion for onset of local necking and Bressan-William's criterion for shear failure. Strain-rate effects are not included in the instability model.

The failure criterion in the subroutine is stress-based and can be written with regards to critical major principle stress:

$$\sigma_1 = \begin{cases} \frac{2K}{\sqrt{3}} \frac{1+\frac{1}{2}\beta}{\sqrt{1+\beta+\beta^2}} \left(\frac{2}{\sqrt{3}} \frac{\hat{\varepsilon}_1}{1+\beta} \sqrt{1+\beta+\beta^2} \right)^n & \text{for } \beta \in (-1, 0] \\ \frac{2}{\sqrt{3}} K \frac{\left(\frac{2}{\sqrt{3}} \hat{\varepsilon}_1 \right)^n}{\sqrt{1-\left(\frac{\beta}{2+\beta}\right)^2}} & \text{for } \beta \in (0, 1] \end{cases}$$

where $\hat{\varepsilon}_1$ is the critical strain and assumed equal to the power law exponent n , and β is the strain increment ratio given as:

$$\beta = \frac{d\varepsilon_2^p}{d\varepsilon_1^p}$$

where ε_1^p and ε_2^p are the major and minor principle plastic strain respectively.

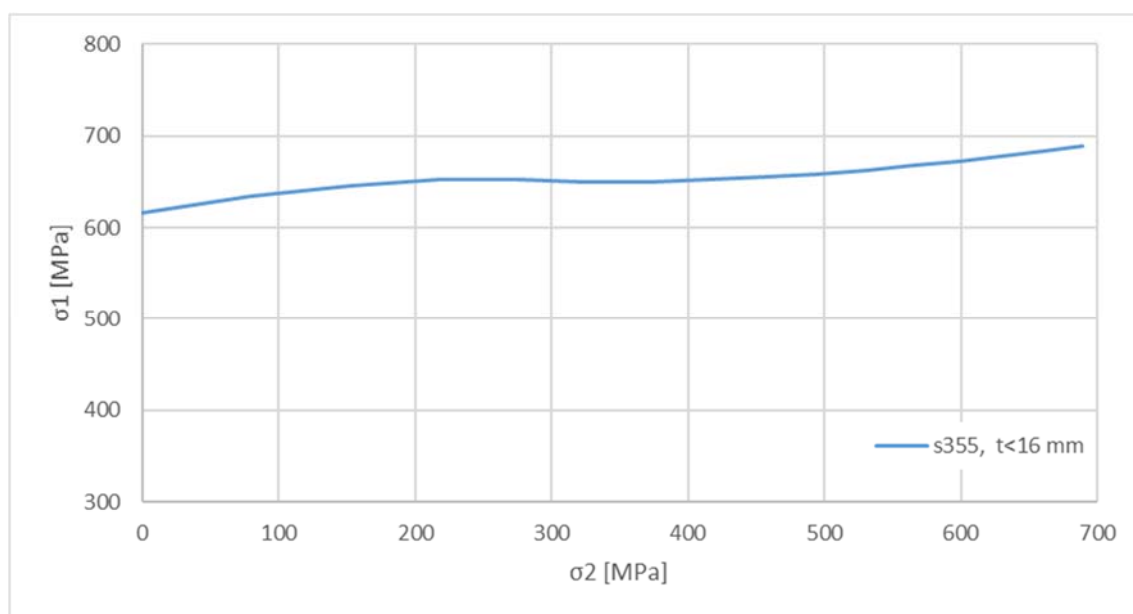


> Figure 3-1 BWH failure criterion for plane-stress conditions. Exemplified with S355 steel.

The parameter $\hat{\varepsilon}_1$ have element size dependent qualities and Alsos et. al. [14] included a scaling factor that have been implemented in the applied subroutine. With the assumption that $\hat{\varepsilon}_1$ equal to n , the mesh scaling is included by doing the following replacement in the expression for σ_1 above:

$$\hat{\varepsilon}_1 = \frac{1}{2} \left(1 + \frac{t_e}{l_e} \right) * n$$

where t_e is the element thickness and l_e is the element length at initial configuration. The effect of this scaling factor has been investigated in section 3.4.2.

3.4 Verification

Verification of the material model is sought through available literature and by comparison with other well-defined material models.

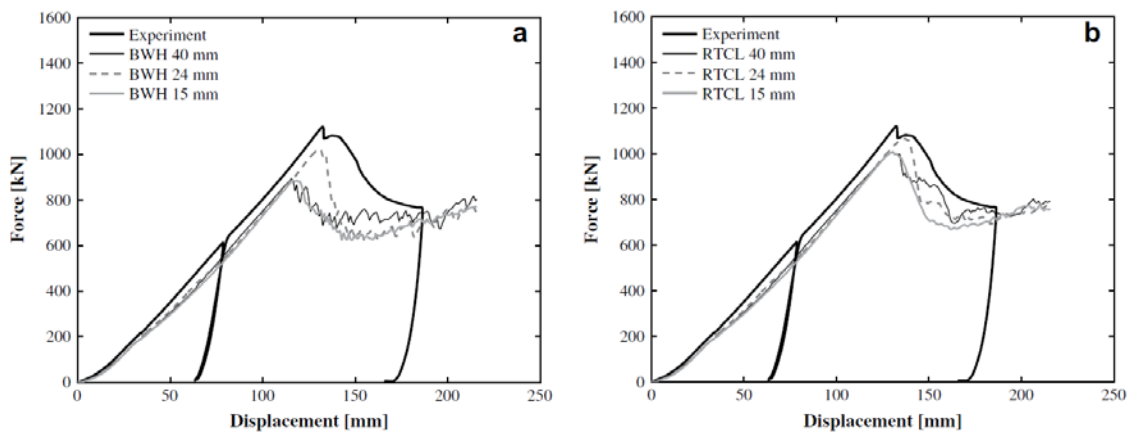
3.4.1 Numerical simulations compared with experimental tests

A study by Alsos, Amdahl and Hopperstad [14] have compared the BWH instability criterion and RTCL fracture criterion with experimental tests presented in [17]. The experimental test is done with a scaled down plate section without stiffeners, with flat bar stiffeners and HP stiffeners. Figure 3-2 show the plate with two HP stiffeners after fracture.



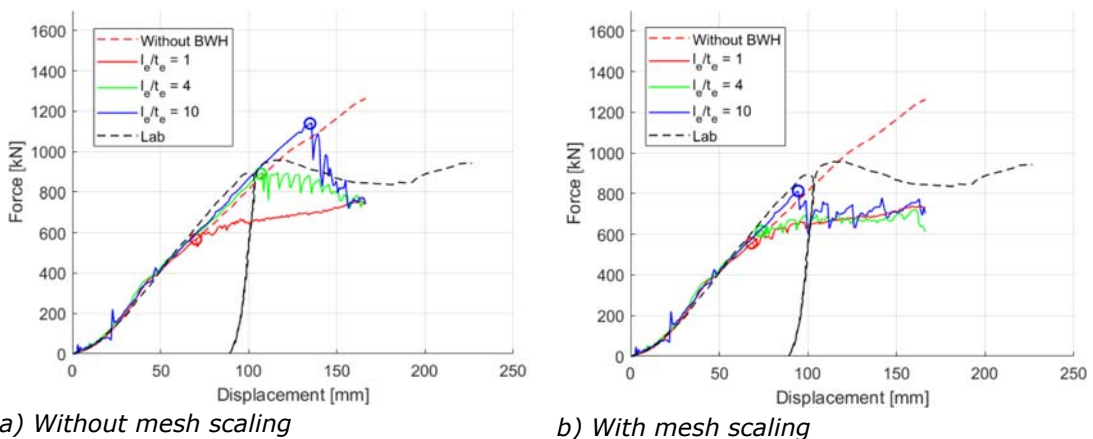
> Figure 3-2 Experimental test. Indentation of panel with 2 HP-stiffeners [17].

Simulations of the plate with two HP stiffeners show that the result is quite mesh dependent for the BWH model, see Figure 3-3. The thickness of the plate is 5 mm and the stiffeners have thickness 6 mm.



- > Figure 3-3 Force-displacement behavior of panel 2-FB. Failure criterion scaling is used at the plate–stiffener junctions: (a) simulations using the BWH criterion, (b) simulations using the RTCL criterion [14]. Plate thickness 40 mm, 24 mm and 15 mm give a l/t -ratio of 8, 4.8 and 3 respectively.

As seen in Figure 3-3 the simulations with the BWH criterion is sensitive to mesh size. Ofstad [9] compared analysis results for the BWH model with both formability tests and the stiffened plate experiment presented by Alsos and Amdahl [17]. Where mesh scaling is applied it is applied for all elements in the model. The simulations show that the mesh scaling underestimate the capacity compared with the experiment presented by Alsos and Amdahl. It should be noted that weld elements are applied in the model. The weld elements get a yield concentration that may occur due to pore element geometry, i.e. length/width ratio. Summary of the results from analysis on the stiffened plate are given in Figure 3-4.



- > Figure 3-4 Force-displacement curves for plate with two HP stiffeners from test and simulations with different mesh size. [9]

Ofstad also apply the BWH model in simulations of the result of another experiment with a stiffened plate subjected to low-velocity impact. This test specimen has 6 L-stiffeners and a planar geometry of 1375 mm x 1250 mm, see [9] for details. In the simulations of this case weld elements are not used. The results show far better agreement with respect to force level at fracture compared with the simulations including weld elements, see Figure 3-5.

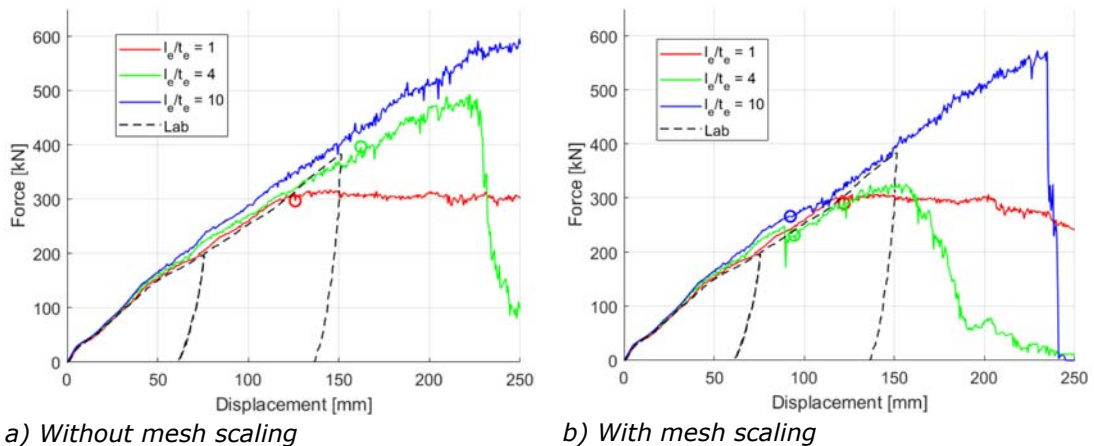


> Figure 3-5 Force-displacement curves for clamped plate with 6 L stiffeners from test and simulations with different mesh size. [9]

From the results discussed above the BWH model is considered suitable for the ship impact analyses performed with mesh scaling applied and no special weld elements.

3.4.2 Sensitivity analyses for material model, effects of mesh size and mesh scaling

To verify the BWH subroutine received from NTNU simulations have been performed on a limited model with the same characteristics as the ship impact models, see Figure 3-6. For more details and additional results see Appendix B [16].

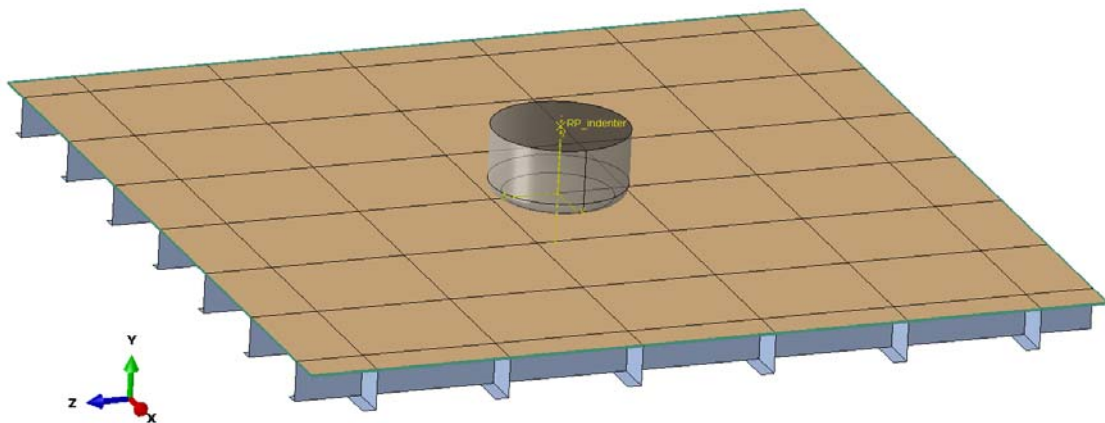


> Figure 3-6 Geometry of model for mesh sensitivity study

The simulations show that the response is sensitive with respect to mesh size. The mesh size influence in particular damage evolution and fracture.

The tested material models FLD (Forming Limit Diagram) and FLSD (Forming Limit Stress Diagram) with Swift instability predict fracture at approximately the same level as BWH without mesh scaling. The FLD material with Store and Rice bifurcation model predict fracture at a higher force level, see Appendix B [16] for material description and results.

The received ship models have typical element-length/thickness (l/t) ratio between 5 and 10 and the same l/t -ration is used when meshing the pontoons and bridge girder.

A mesh sensitivity study is performed for l/t -ratios from 1 to 50.

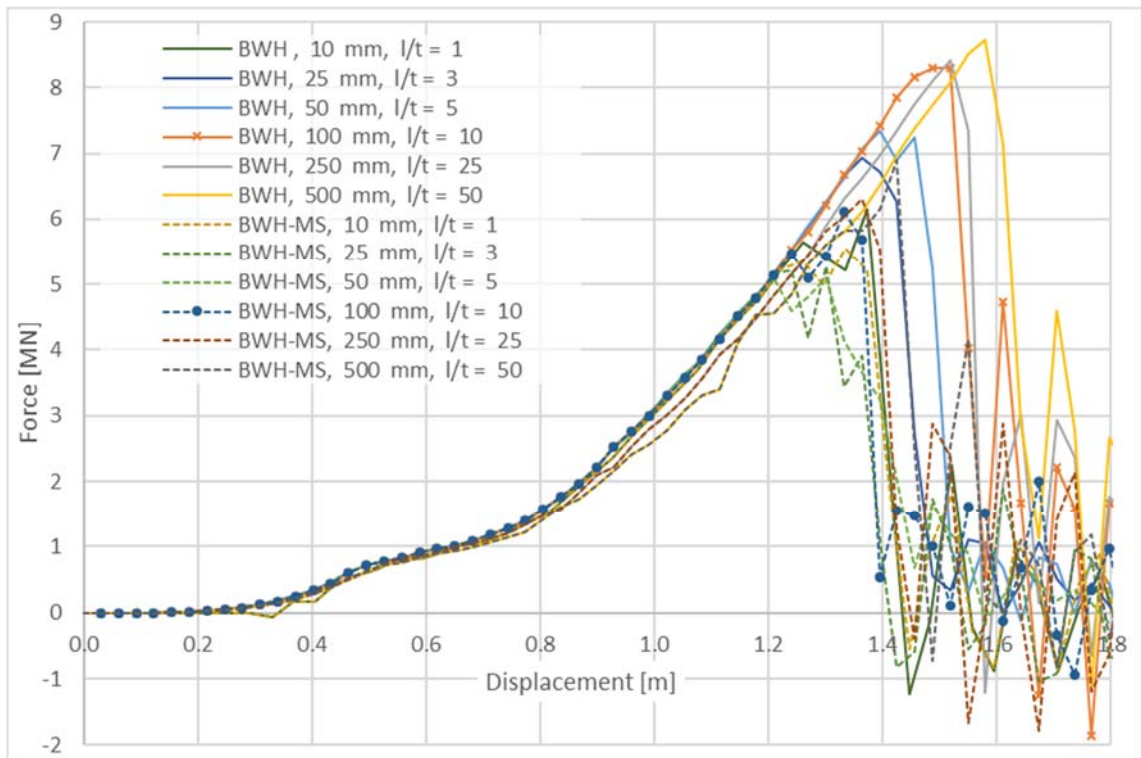


> Figure 3-7 Sensitivity study for BWH. MS – mesh scaling.

The difference in force level at collapse is more significant in simulations using materials without mesh scaling than for the simulations where mesh scaling is applied. The results for $l/t=1$ without mesh scaling is in the same range as results with mesh scaling and l/t -ratio of 1-25.

With respect to the effect of mesh size it is chosen to use the BWH model with l/t -ratio of 5-10 and apply mesh scaling to the full analysis.

4 SIMULATION MODELS

The software Abaqus/Explicit [8] is utilized for the local ship impact analyses.

4.1 Geometry

The simulation models for local response of deckhouse-girder collision consist of two parts, a ship with deckhouse and a bridge girder.

A representative ship deckhouse model is provided by the Client and described in the Design Basis [1].

The geometry of the bridge girder is taken from the K7 end-anchored floating bridge in phase 3 of the Bjørnafjorden project, drawing K7-031 [18]. It is chosen to model the standard bridge girder cross section, i.e. the cross section for the low bridge, because a weaker cross section is considered conservative in terms of damage to the bridge girder.

A reinforced bridge girder cross section with equal plate and stiffener thicknesses as the cross section in drawing no. SBJ-33-C5-OON-22-DR-142-B [19] is controlled to reflect the final design (drawings [20] [19]) and to check if the reinforced bridge girder cross section results in higher force and energy level or damage to the bridge girder.

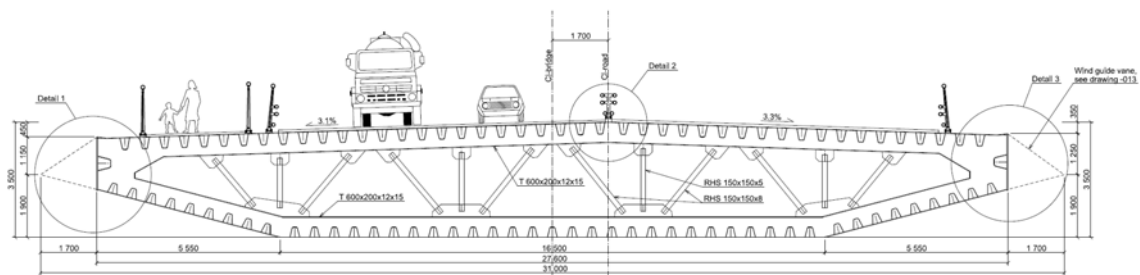


> Figure 4-1 Plan of the standard bridge girder cross section, from drawing K7-031 [18]

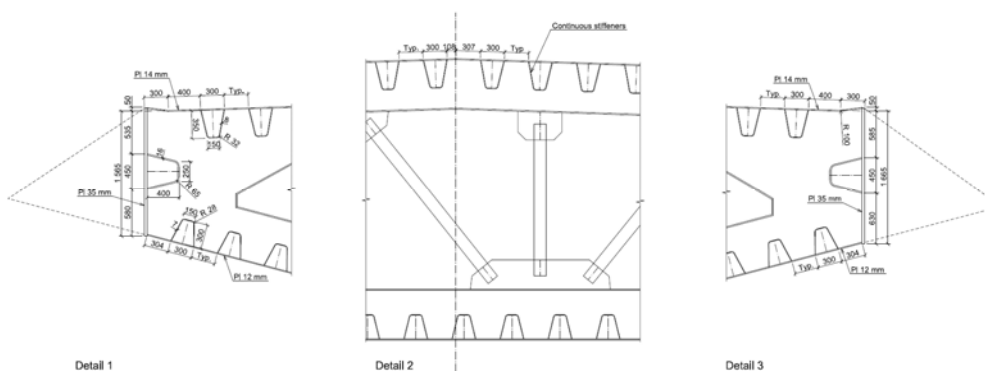


> Figure 4-2 Details of the standard cross section, from drawing K7-031 [18]

Bridge girder finite element model data overview (not final design):

- Length modelled: 44 m (11 sections between transverse girders)
- Plate thicknesses: 14 mm (top), 35 mm (side walls), 12 mm (bottom)
- Stiffeners: 8 mm (top), 16 mm (side walls), 7 mm (bottom)
- Transverse girders: 600x200x12x15
- Bracings in transverse girders: RHS 150x150x5 vertical / RHS 150x150x8 diagonal

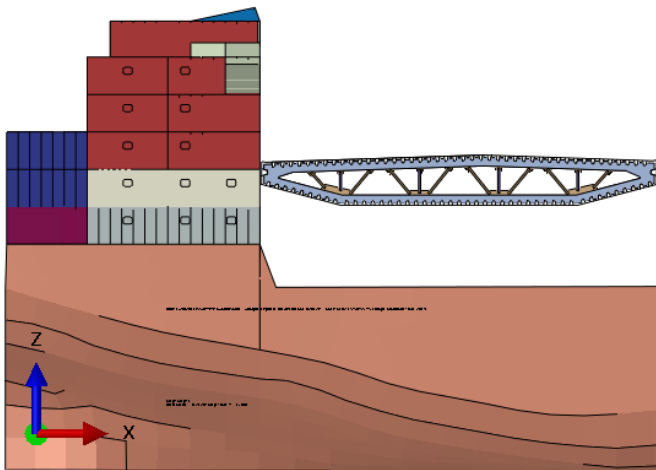


> Figure 4-3 Deckhouse ship and bridge girder finite element model, impact at deck 2

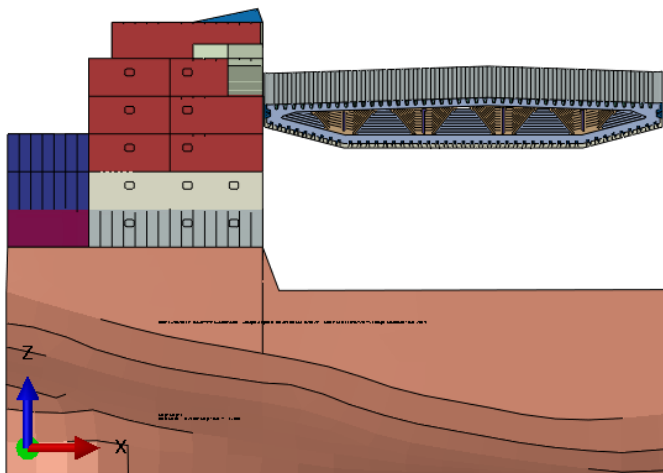


> Figure 4-4 Deckhouse ship and inclined bridge girder finite element model, impact at deck 4

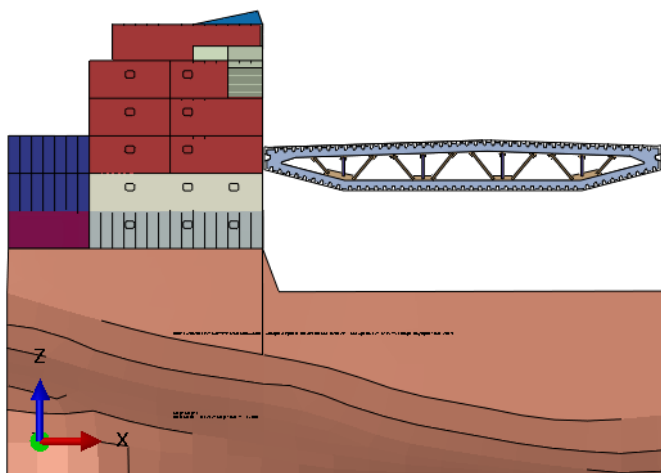


> Figure 4-5 Deckhouse ship and bridge girder finite element model, impact between deck 2 and 3

The modelled length of the bridge girder is considered sufficiently for local response investigation since the stresses are in the elastic area at the boundaries.

4.2 Materials

It has been performed a large amount of sensitivity analyses related to material model and material quality. With reference to chapter 3, the Bressan-Williams-Hill (BWH) instability criteria is considered as the most reliable material model tested.

Mainly two sets of material parameters to define the isotropic hardening have been utilized in the analyses:

1. *Low deckhouse, low bridge girder*: Low fractile material parameters according to DNVGL-RP-C208 [6] section 4.6.6
2. *Mean deckhouse, low bridge girder* (but higher than low bridge girder in bullet 1): "Mean-low" material parameters with
 - a. Yield stress according to DNVGL-RP-C208 [6], mean value of S275 (section 7.8) and low fractile value of S355 and S420 (section 4.6.6)
 - b. $\epsilon_{\text{plateau}}$ according to DNVGL-RP-C208 [6] (sections 4.6.6 and 7.8)
 - c. Hardening parameters K and n based on formulas mentioned by Storheim [21] section 3.7.3:

$$n = \ln(1 + \epsilon_{\text{UTS}} - \epsilon_{\text{plateau}})$$

$$K = \sigma_{\text{UTS}} \cdot \left(\frac{\epsilon}{n}\right)^n$$

where ϵ_{UTS} is the maximum uniform strain (elongation) from a tensile test and σ_{UTS} is the associated ultimate tensile strength

- d. ϵ_{UTS} and σ_{UTS} from DNVGL-OS-B101 [7]

The material parameters in bullet number 2 are summarized in Table 4-1. Figure 4-6 shows the evaluated stress-strain curves. True stress-strain curves are utilized as oppose to engineering stress-strain curves.

> Table 4-1 "Mean-low" material parameters

	Steel quality	Yield stress ¹	$\epsilon_{\text{plateau}}$	K	n
Deckhouse	S275	331.8 MPa	0.017	764 MPa	0.185
Bridge girder	S420	422.5 MPa	0.012	827 MPa	0.155

¹ For thicknesses 16 mm and below

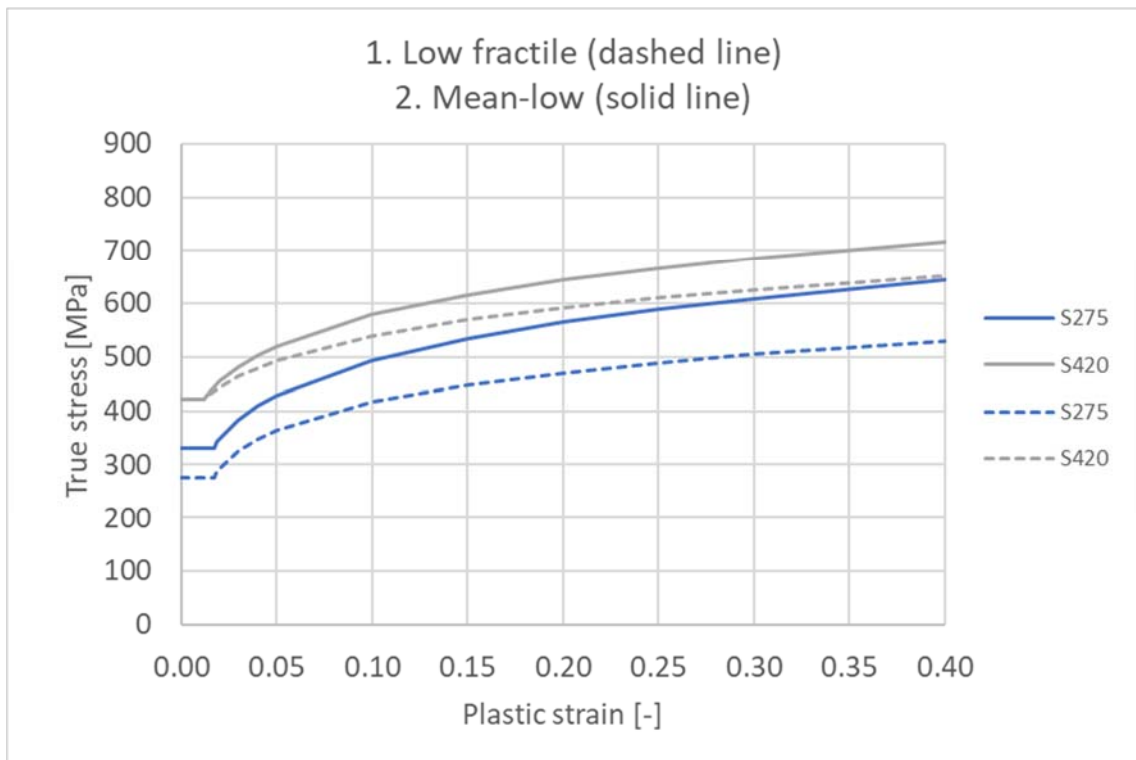


> Figure 4-6 True stress-strain curves of the steel materials, solid lines define the base case materials utilized

Mean material parameters according to DNVGL-RP-C208 [6] have also been tested. In addition, a set of “mean-high” material parameters with mean yield stress (according to [6]) and high K for S355 and S420, is tested. Yield stress, $\epsilon_{\text{plateau}}$ and K for S275 in the “mean-high” set of material parameters are equal to S275 in Table 4-1. See Appendix C section 1 [22] for details.

The reason for choosing low yield stress and K for the bridge girder is because the “mean-high” material parameters are considered too conservative. Note that the low values chosen are still higher than low fractile values according to DNVGL-RP-C208 [6]. Since the bridge is designed utilizing low material properties, it seems more holistic to utilize low material properties for the bridge girder when evaluating the ship impact response. The “mean-low” material parameters are furthermore close to the material parameters chosen for the work performed at NTNU [13] and by the suspension bridge group [15] in the previous phases of the Bjørnafjorden project.

The choice of material parameters defining the isotropic hardening can affect the ship impact response significantly. Generally, a higher material curve also represents a higher force and energy level. To lower the uncertainties regarding higher material quality than accounted for, an opportunity is to specify the maximum values to yield and ultimate tensile stress to the supplier of the bridge steel materials. This is checked with SSAB that it is possible [23]. SSAB also states that typical maximum yield strength for S420 is 40-60 MPa above minimum value [23]. Minimum and maximum tensile strength is usually specified in the supplier’s data sheets or standards, for example DNVGL-OS-B101 [7].

Following material characteristics are also utilized for the simulations:

- Mesh scaling as a part of the BWH model, described in section 3.3 and 3.4, is applied to the entire model.
- Young's modulus $E = 210 \text{ GPa}$, Poisson's ratio $\nu = 0.3$ and density $\rho = 7850 \text{ kg/m}^3$ are chosen for all materials.

4.3 Mesh and element formulations

The finite element model consists of mainly S4R elements, which are linear shell elements with reduced integration. A few S3R elements occur. Full integration for all triangular and rectangular elements in the finite element model is tested for sensitivity analysis.

The characteristic element size of the deckhouse ship model is 100 mm. The element size of the stiffeners in the deckhouse is 80-140 mm, with typically one-two elements over the height of the stiffener.

For the bridge girder model, the characteristic element size is 100 mm at impact areas. The element size of the stiffeners in the bridge girder model is 90-110 mm, with typically three-five elements over the height of the stiffener.

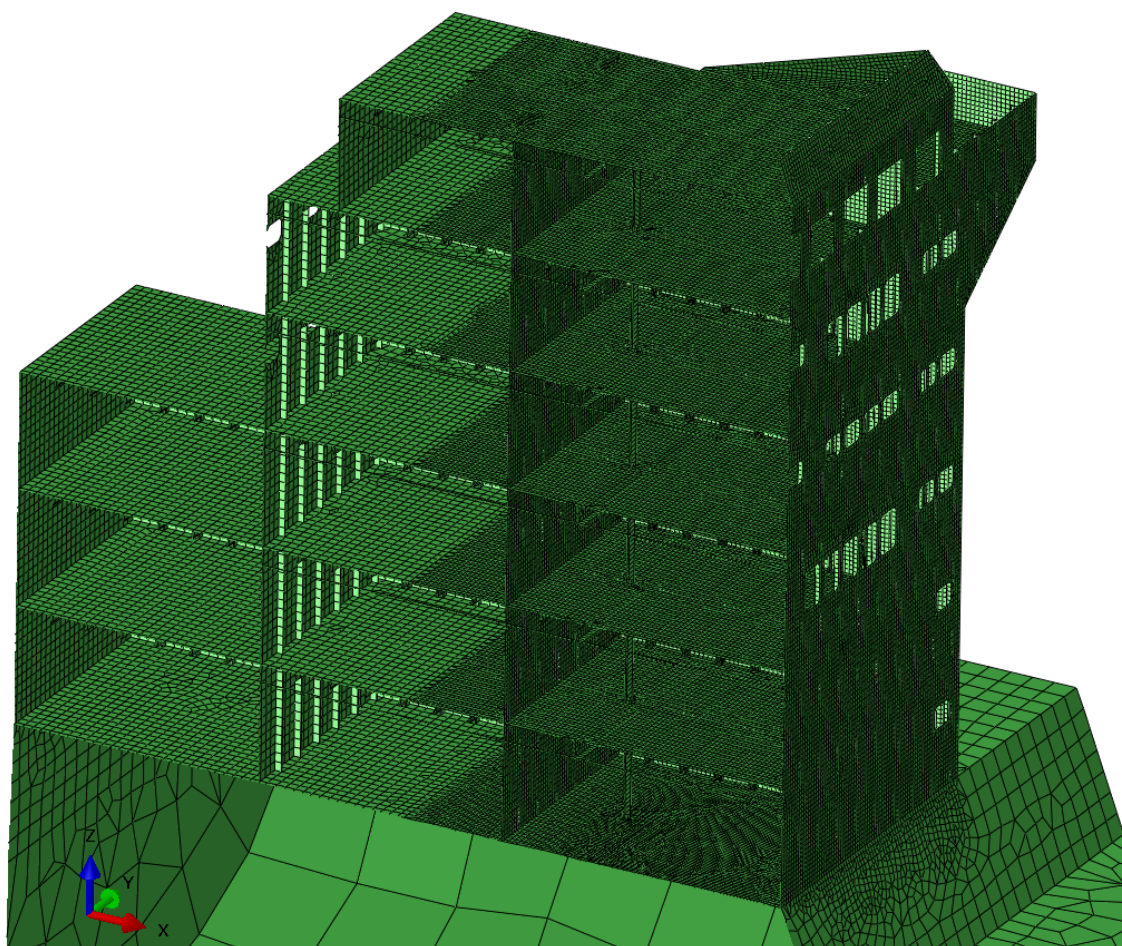


> Figure 4-7 Mesh of the deckhouse ship, shown cut in half

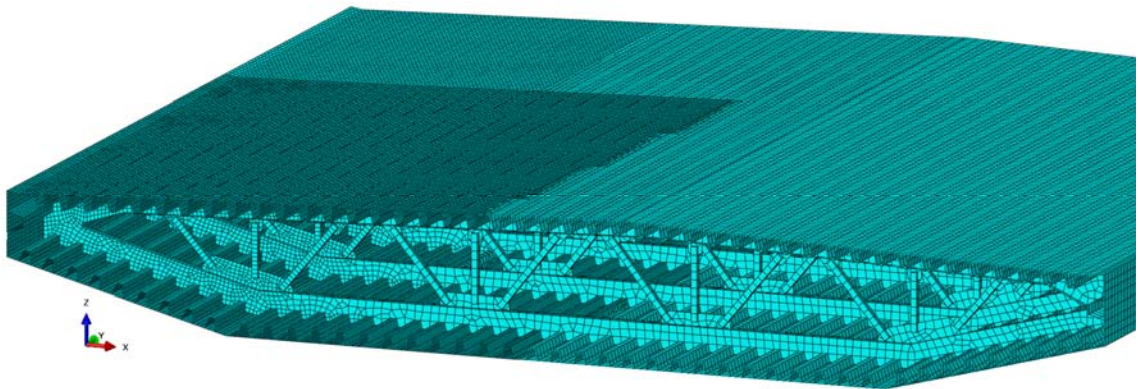


> Figure 4-8 Mesh of the bridge girder, shown cut in half

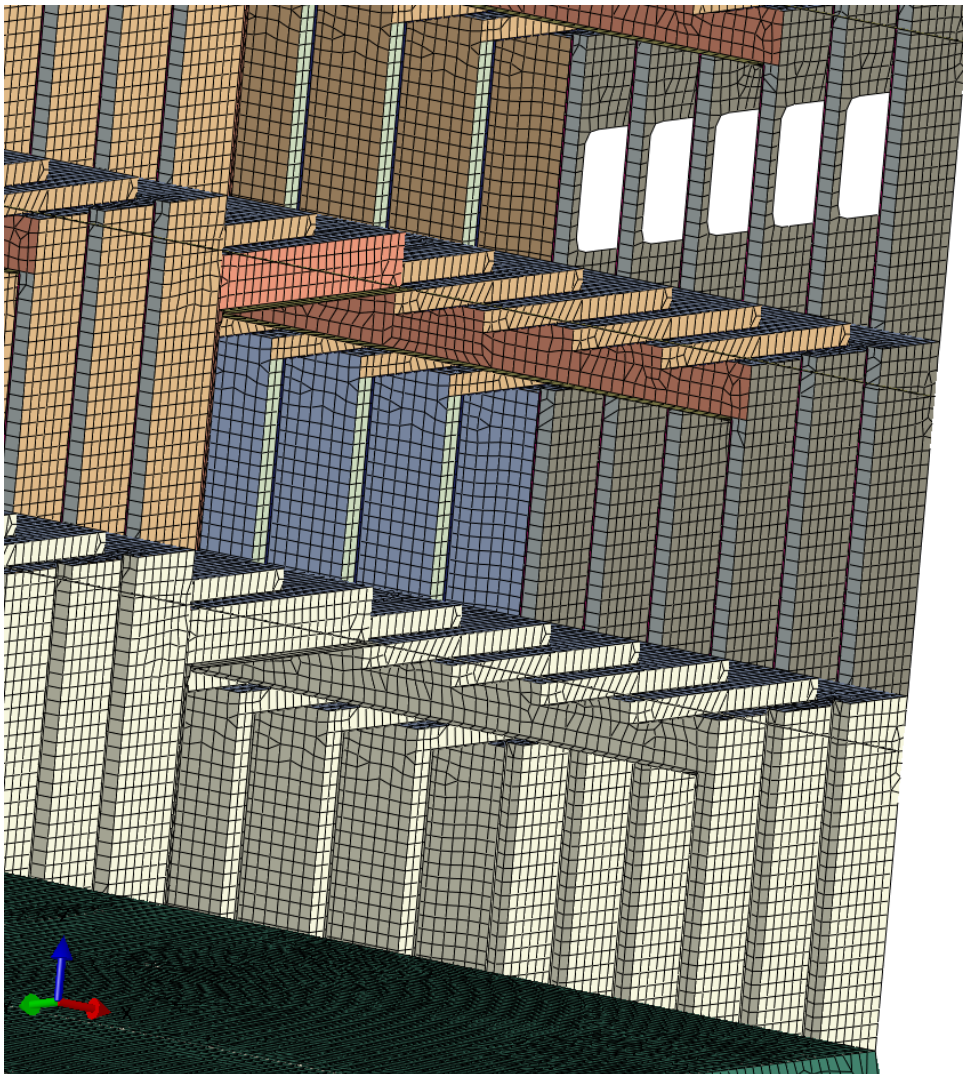


> Figure 4-9 Detailed mesh of the deckhouse ship

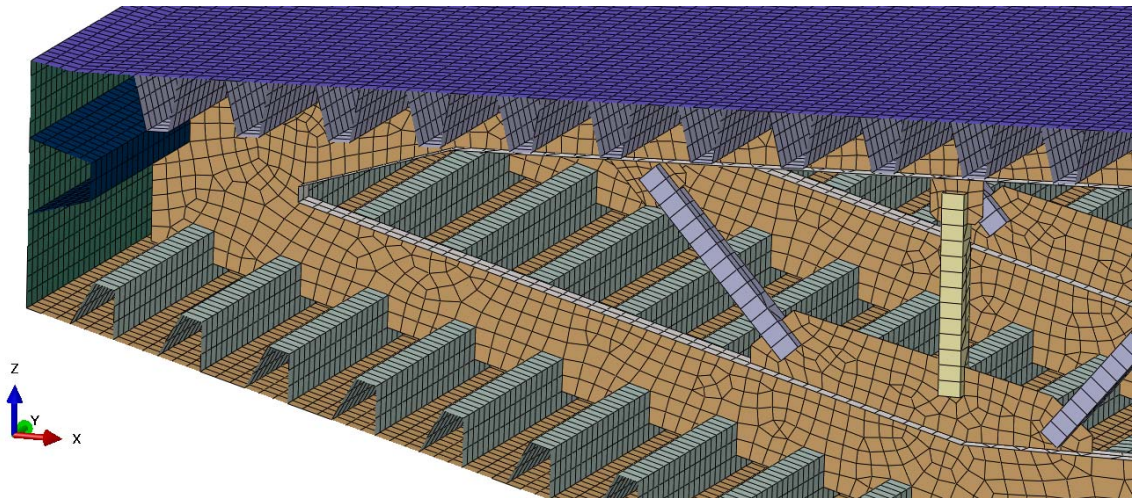


> Figure 4-10 Detailed mesh of the bridge girder

4.4 Analysis setup

4.4.1 Boundary conditions

The bridge girder is modelled fixed at the boundary cut-offs as illustrated in Figure 4-11. The cut boundaries are constrained with kinematic couplings to reference points. Fixed boundaries are satisfactory to use because the stresses at the boundary are low, see section 5.3.1.

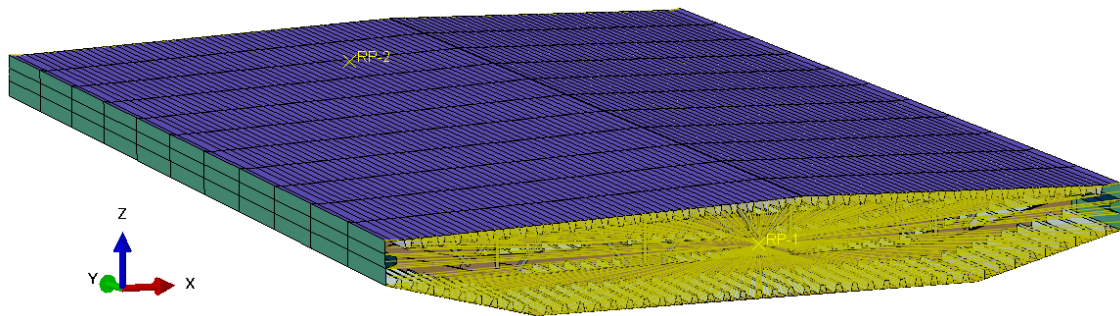


> Figure 4-11 Boundary condition at the cut-off boundary of the bridge girder

Boundary conditions for the deckhouse ship are shown in Figure 4-12. The deckhouse ship is fixed in all rotational degrees of freedom in a reference point in the hull of the ship. The hull is constrained as a rigid body to the reference point.

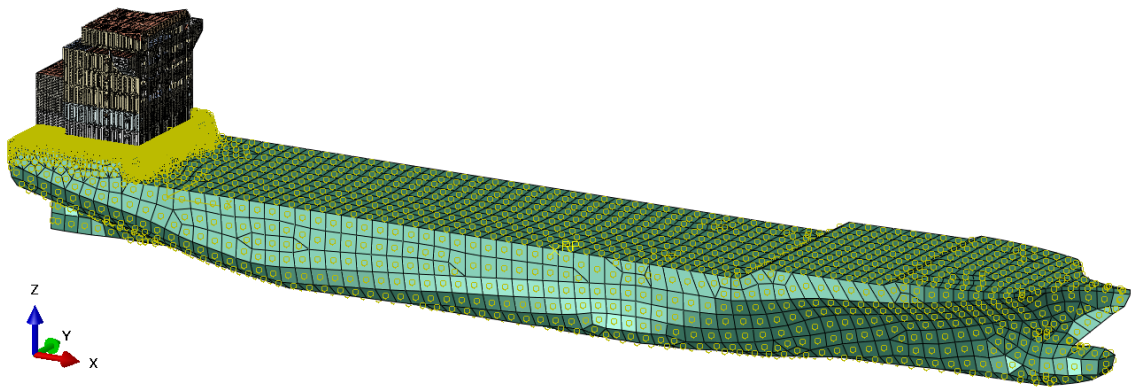


> Figure 4-12 Boundary condition in the hull of the deckhouse ship

4.4.2 Loads

The only load applied in the simulations models is velocity to the deckhouse ship. This is performed in two steps prior to the impact to avoid unwanted dynamic effects. In step one, velocity is applied to the entire deckhouse ship model. In step two, the velocity is "turned off" for the deckhouse, while velocity is still applied to the hull. The deckhouse will move towards the bridge girder which happens in step three.

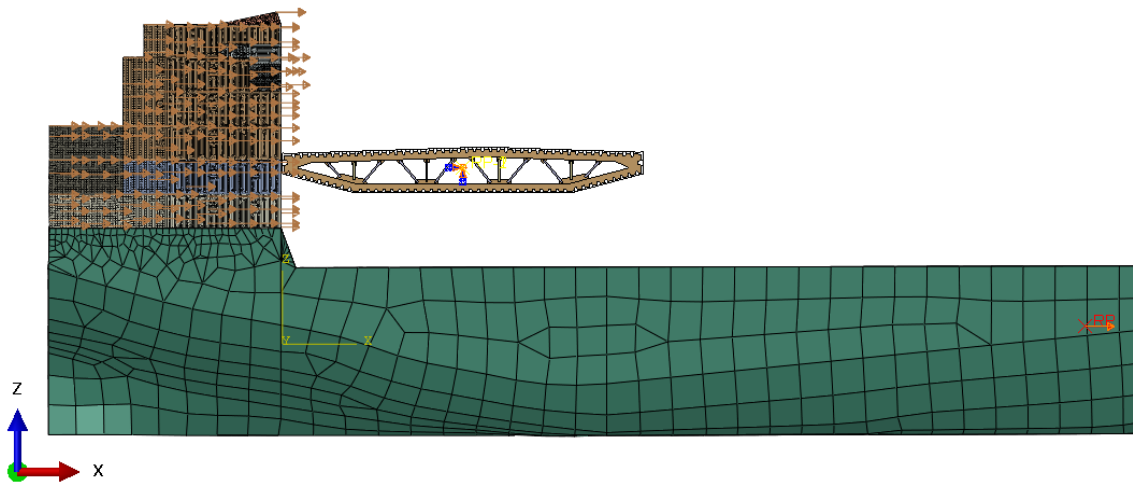


> Figure 4-13 Velocity applied to the deckhouse ship in step one

4.4.3 Interactions

A general contact condition is applied to the entire model, including both sides of the surface of all elements in the model. The normal behavior is "hard" contact and the friction coefficient is 0.3.

4.4.4 Output parameters

Output parameters of interest are:

- *Contact force*: Total force due to contact pressure
- *Frictional dissipation*: Frictional dissipated energy

- *Strain energy*: Elastic strain energy
- *Plastic dissipation*: Inelastic dissipated energy
- *Artificial energy*: Artificial strain energy related to hourglass control and drilling rotation control
- *Internal energy*: Or total strain energy. For the simulations in this report, the internal energy is the sum of strain energy, plastic energy and artificial energy.

4.4.5 Analysis setup for residual capacity model

It is desired to study the strength of the bridge girder after a ship impact. The residual capacity is evaluated by applying rotations at the cut-off boundaries of the bridge girder, see Figure 4-14.

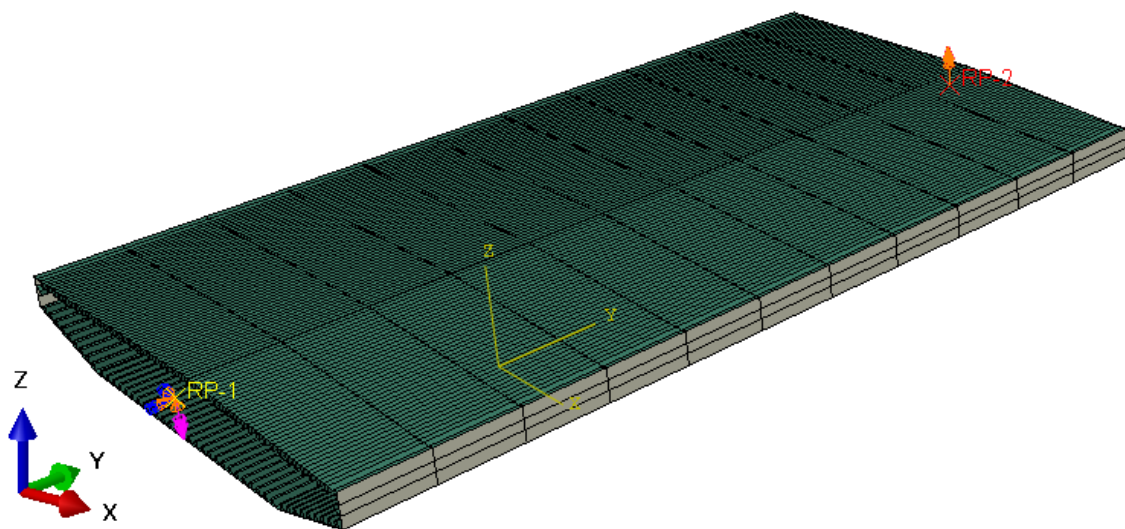


> *Figure 4-14 Rotation about strong axis applied to the cut-off boundaries of the bridge girder*

This is performed for the intact bridge girder and for the damaged bridge girder after corresponding 4 m, 8 m, 12 m and 16 m ship displacement. Stresses and deformations from the ship impact analysis are preserved for the residual evaluation.

The material and mesh of the girder is equal to the girder from the ship impact analysis. Imperfections are not included; this is not necessary as the goal is to compare the capacity of the damaged girders.

Since the BWH material model utilized for the ship impact analyses is limited to the explicit solver, residual capacity of the damaged bridge girders must also be evaluated with the explicit solver.

5 SIMULATIONS

5.1 Load cases

Table 5-1 gives the impact energy for the bridge girder. This energy is to be dissipated locally and globally for a collision event.

> *Table 5-1 Impact energy for bridge concept K12, CC 100 m and 125 m*

Element	Displacement	Velocity	Impact energy ²
Bridge girder	19 084 ton	6.2 m/s	385 MJ

Table 5-2 gives the base impact cases for local response of deckhouse-girder collision. Ships with deckhouse can collide with the bridge girder due to the height of the deckhouse. Different impact locations have been investigated.

> *Table 5-2 Impact scenarios deckhouse-girder collision*

Load case	Type of ship	Impact location	Comment
A	Deckhouse	At deck 2	11.5 m clearance to water level
B	Deckhouse	Inclined at deck 4	High bridge
C	Deckhouse	Between deck 2 and 3	

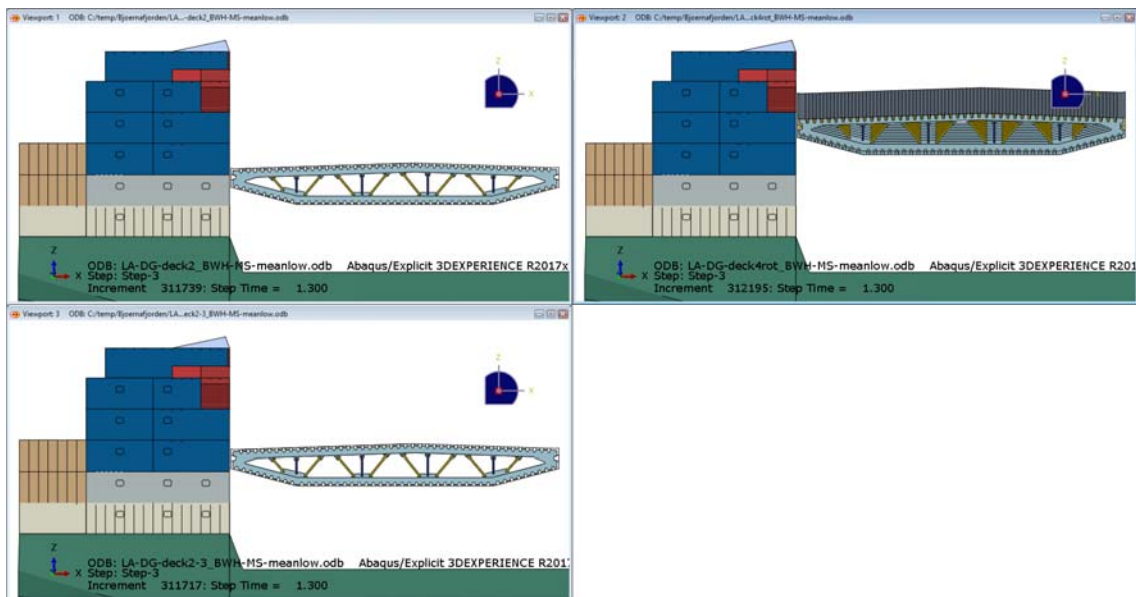


> *Figure 5-1 Load cases A-C of deckhouse-girder collision side view: At deck 2 (upper left), inclined at deck 4 (upper right), between deck 2 and 3 (lower left)*

² Included 5 % added mass

Sensitivity analyses have been performed related to material model, material quality and mass scaling.

5.2 Response parameters

The goal of the local response simulations is to evaluate the force-displacement curves for load input to the global response simulations [24].

The extent of damage to the bridge girder is also obtained from the local simulations. This must be calibrated with the global simulations to reaffirm the amount of energy that is dissipated locally.

When the local damage is known, reduced stiffnesses and capacities (reduced section modulus or second moment of inertia) can also be given as input to evaluate the damaged condition with a 100-year environmental loading applied to the bridge.

5.3 Response

5.3.1 Damage illustrations of base impact cases

Figure 5-2 to Figure 5-3 show the deckhouse and bridge girder damage for the load cases in Table 5-2 at 8 m ship displacement. The deckhouse is subjected to severe damage for all impact locations, while damage to the bridge girder is limited. Deformations are not scaled.

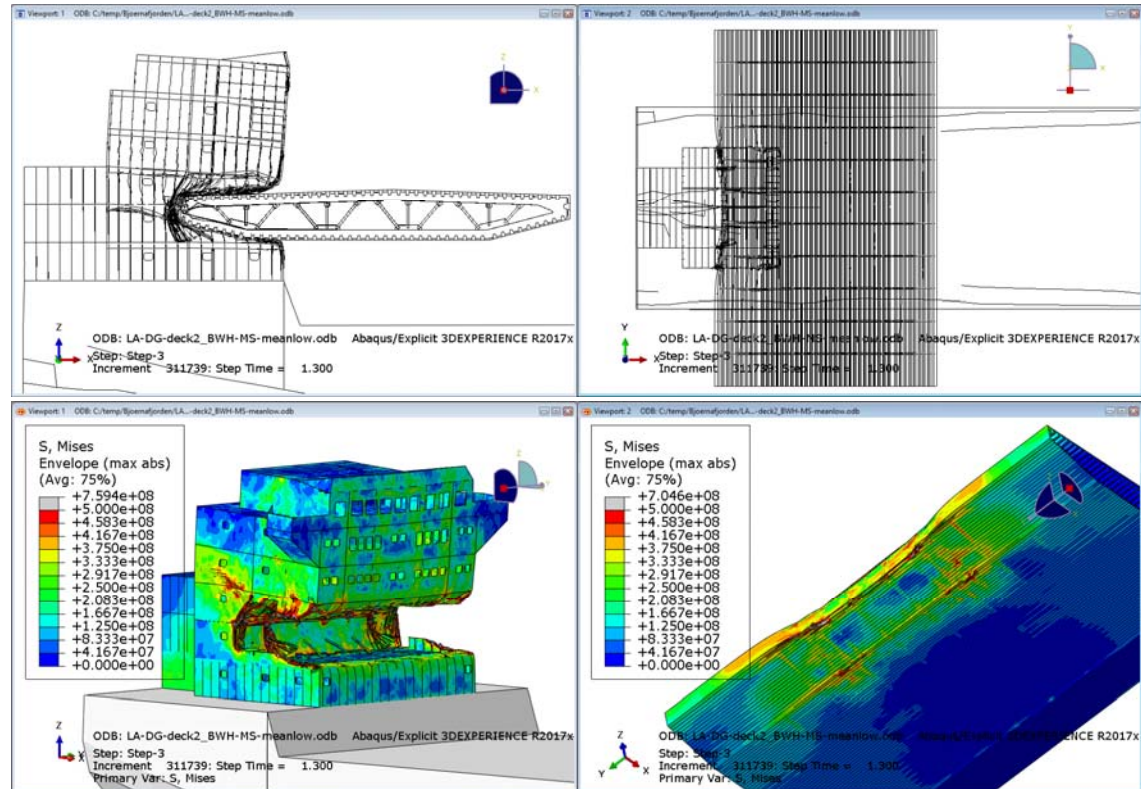


> Figure 5-2 von Mises stress [MPa] load case A: Bridge girder at deck 2

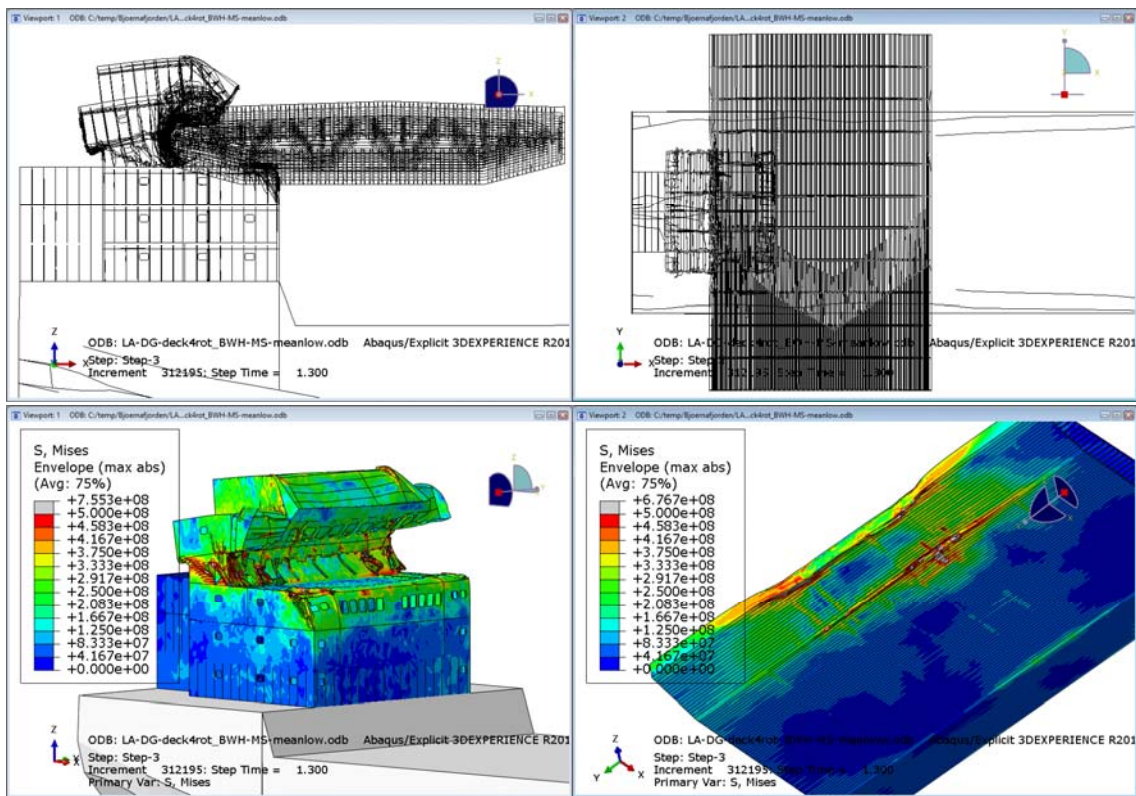


> Figure 5-3 von Mises stress [MPa] load case C: Bridge girder inclined at deck 4

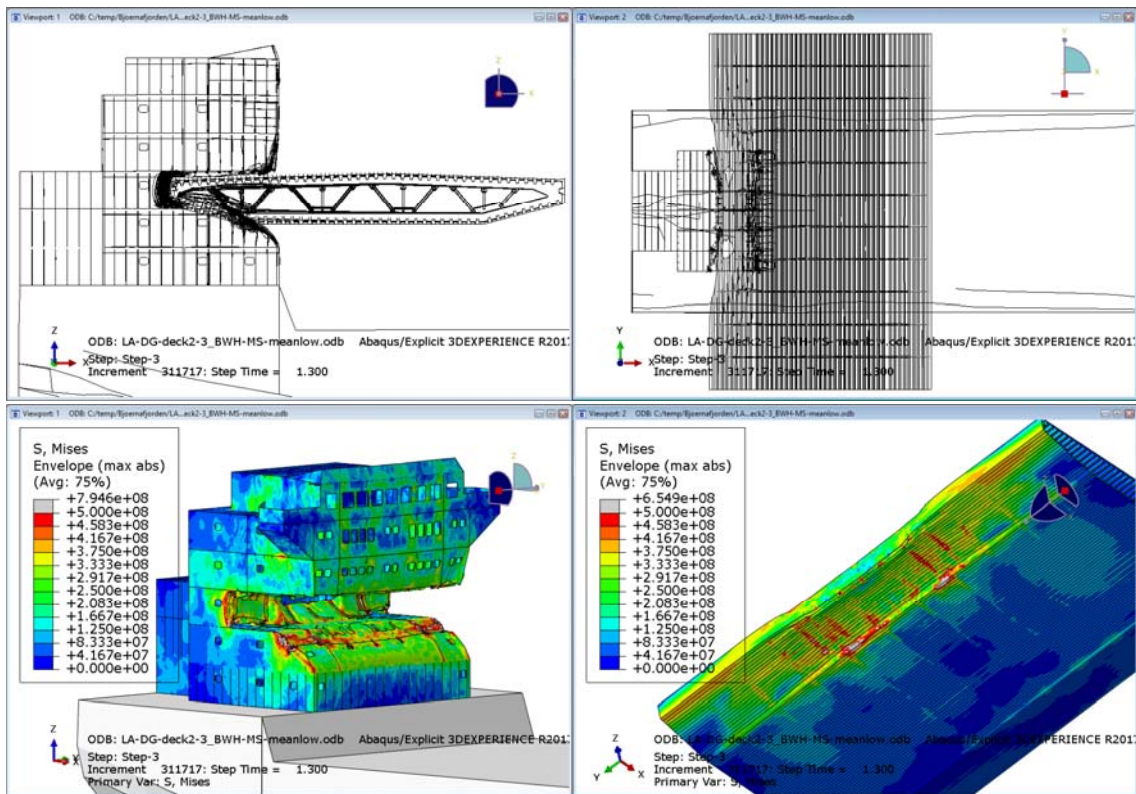


> Figure 5-4 von Mises stress [MPa] load case B: Bridge girder between deck 2 and 3

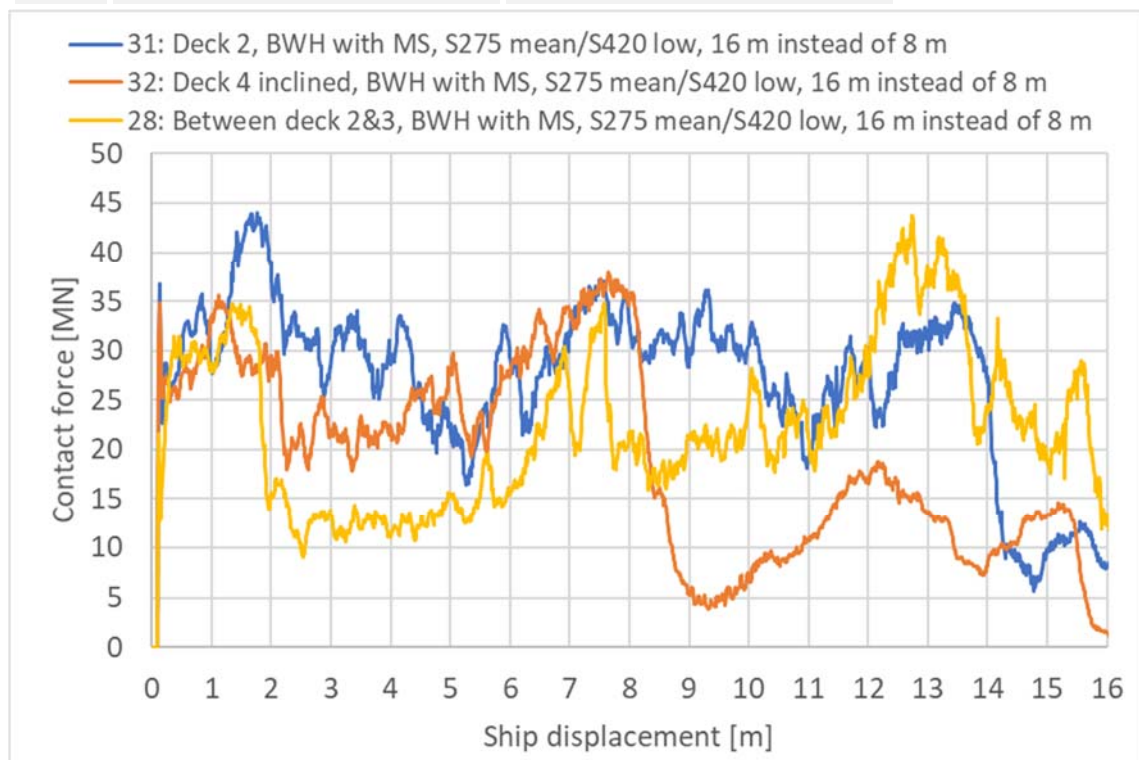
5.3.2 Base impact cases

Figure 5-5 shows the force-displacement curves for the load cases in Table 5-2 with “mean-low” material parameters described in section 4.2. The maximum and mean contact force is for comparison given for the period up to 8 m ship displacement.

The impact force level is higher when the bridge girder is hit at a deck level. If the bridge girder is hit between two decks, the impact force is much lower. Impact low on the deckhouse results also in higher force level because the deckhouse is stiffer close to the hull.

A peak which is not realistic is seen when the bridge girder is hit at a deck level. This peak reduces significantly if the bridge girder is hit between two decks. The peak is due to the hard contact definition in the model and manifests when the stiff deck and the stiff bridge girder hits perfectly normal to each other.

ID-no.	Max. contact force [MN] 0-8 m	Mean contact force [MN] 0-8 m
31	44	30
32	38	27
28	35	20



> Figure 5-5 Contact force [MN] impact deckhouse-girder

Figure 5-6 shows the internal energy dissipated in the deckhouse with dashed line and the bridge girder with solid line. Here, the internal energy is the sum of strain energy, plastic dissipation and artificial energy. The largest proportion of the internal energy is the plastic dissipation.

It is seen that the deckhouse dissipates most of the energy. Impact at a deck level causes significantly faster energy dissipation in the deckhouse than when the impact location is between the decks, reflecting the area under the force-displacement curve. The internal energy in the bridge girder is low for all impact locations. For impact at a deck level the dissipated energy in the bridge girder stabilizes, while impact between two decks causes a slight increase of the dissipated energy in the girder. The impact energy to be dissipated in the bridge girder is 385 MJ. The local dissipated energy does not reach this level at 8 m ship displacement.

A stabilization of the dissipated energy in the bridge girder indicates that a reinforced cross section will not change the results much; the bridge girder is already very stiff compared to the deckhouse.

Figure 5-7 shows the frictional dissipation and artificial energy in the models. The proportion of artificial to internal energy is 8-10 % for the displayed models. The artificial energy reduces when utilizing elements with full integration, but this is time demanding.

The effect of reduced integration is investigated in Appendix C section 3 [22].

Figure 5-8 shows that the proportion of internal energy dissipated in the bridge girder is moderate for all load cases. Impact between deck 2 and 3 with displays a bit higher energy dissipation in the girder.

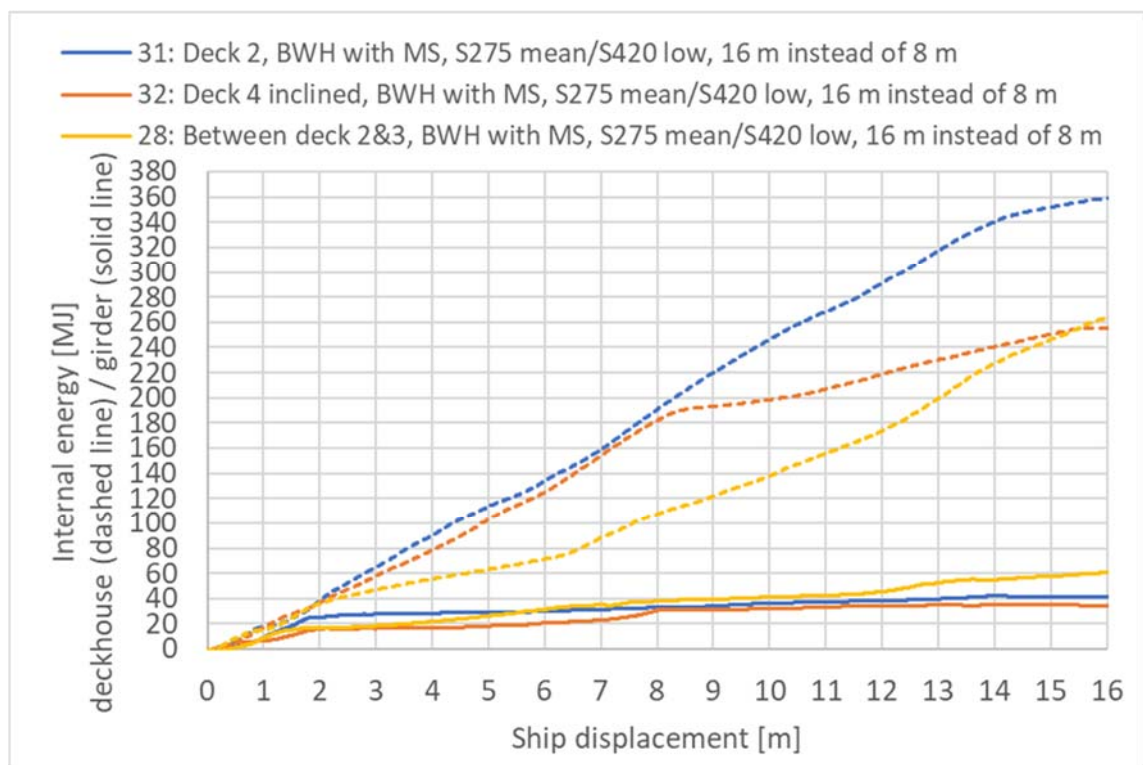


> Figure 5-6 Internal energy [MJ] impact deckhouse-girder

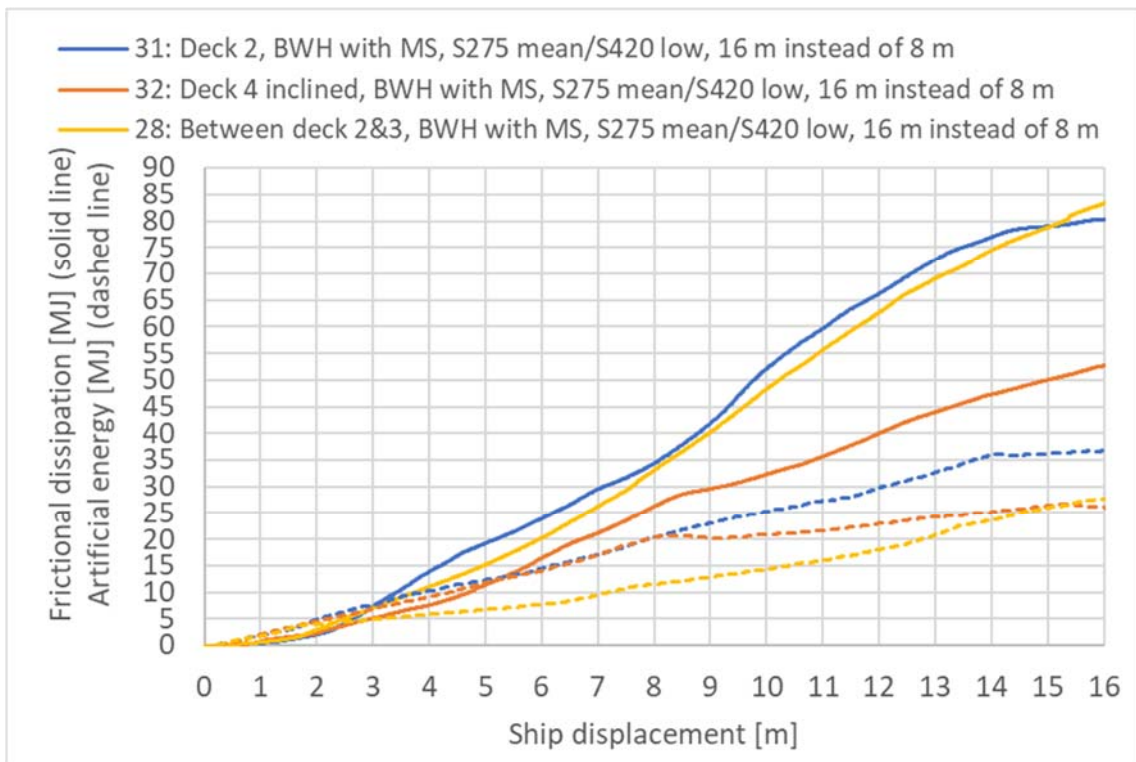


> Figure 5-7 Frictional dissipation and artificial energy [MJ] impact deckhouse-girder

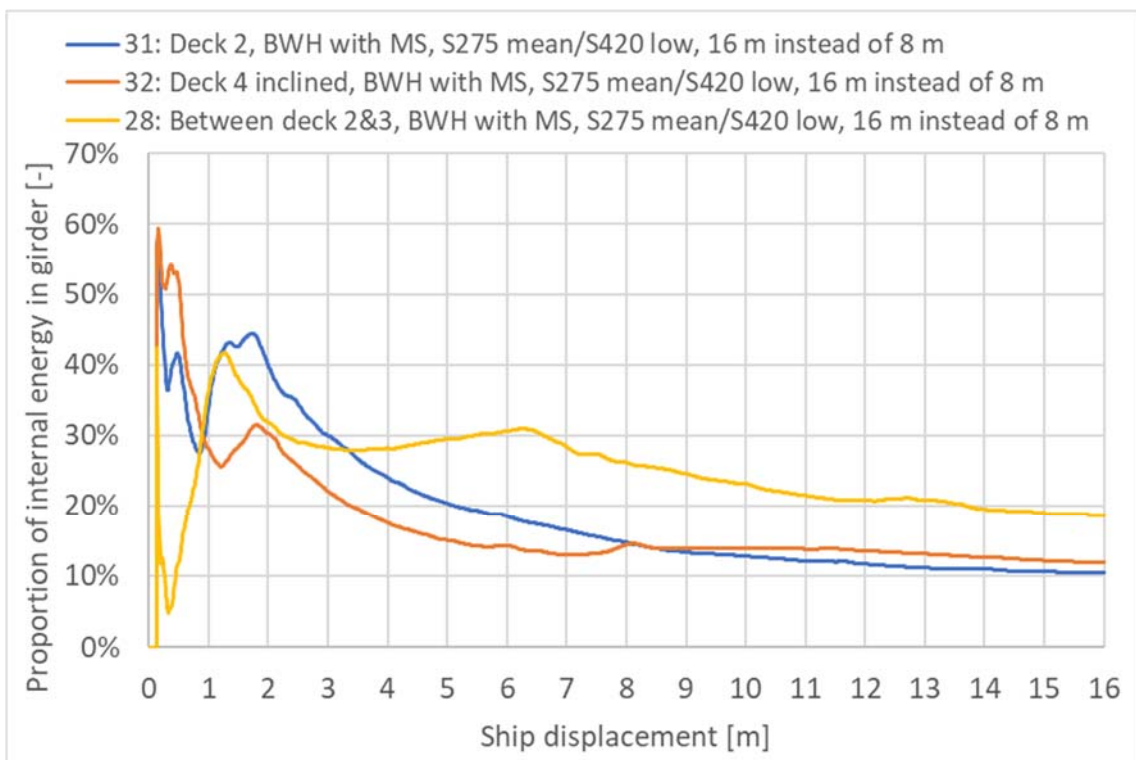
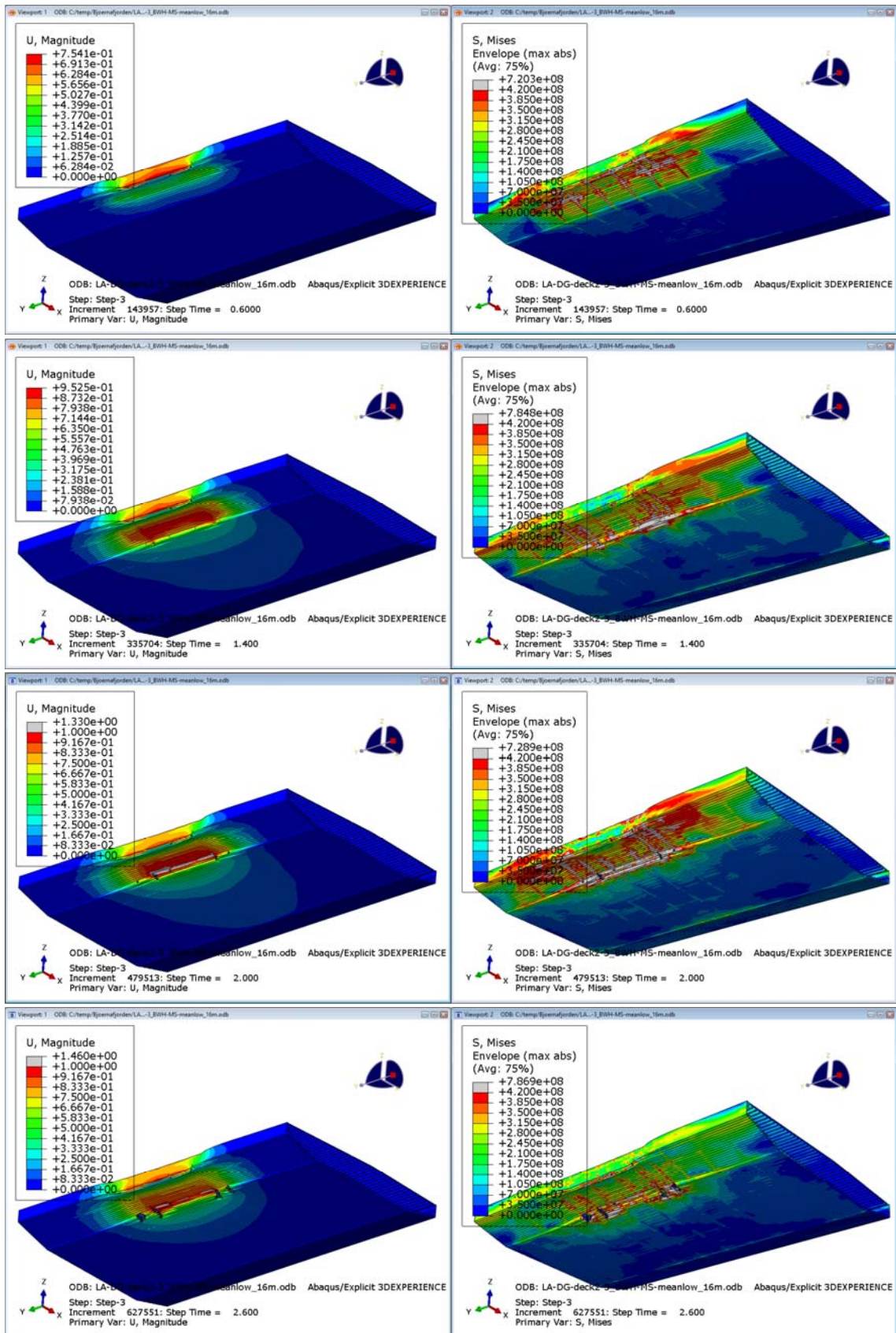


> Figure 5-8 Proportion of internal energy in girder [-] impact deckhouse-girder

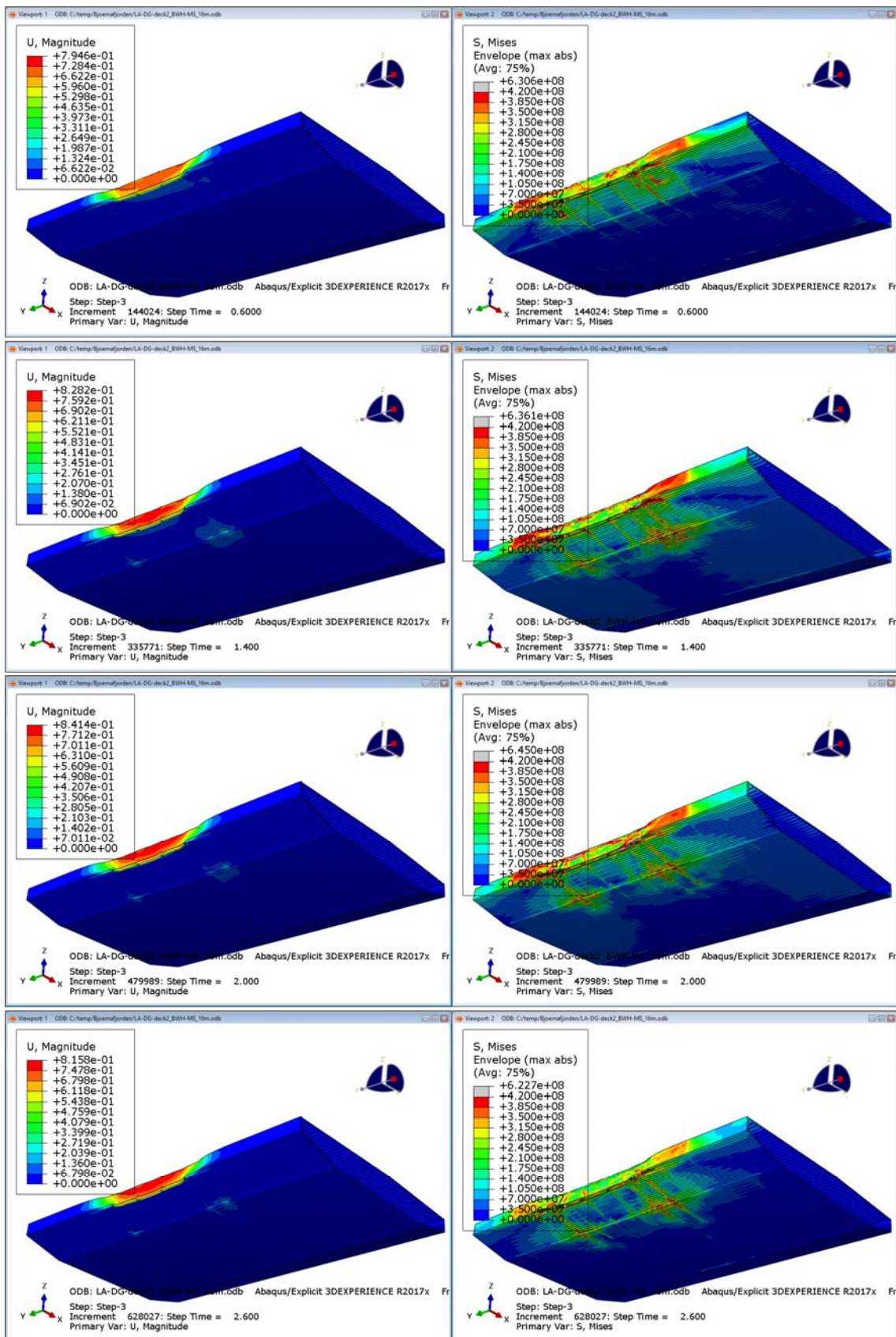
5.3.3 Residual capacity of bridge girder

Figure 5-9 shows the damaged bridge girder from local response of deckhouse-girder collision between deck 2 and 3, while Figure 5-10 is from collision at deck 2. The damaged girder from collision between deck 2 and 3 is the basis for the residual capacity evaluation of moment about strong axis, while the damaged girder from collision at deck 2 is the basis for the residual capacity evaluation of moment about weak axis. The reason for the different bases is because these locations resulted in the lowest capacities for the respective unit moments.

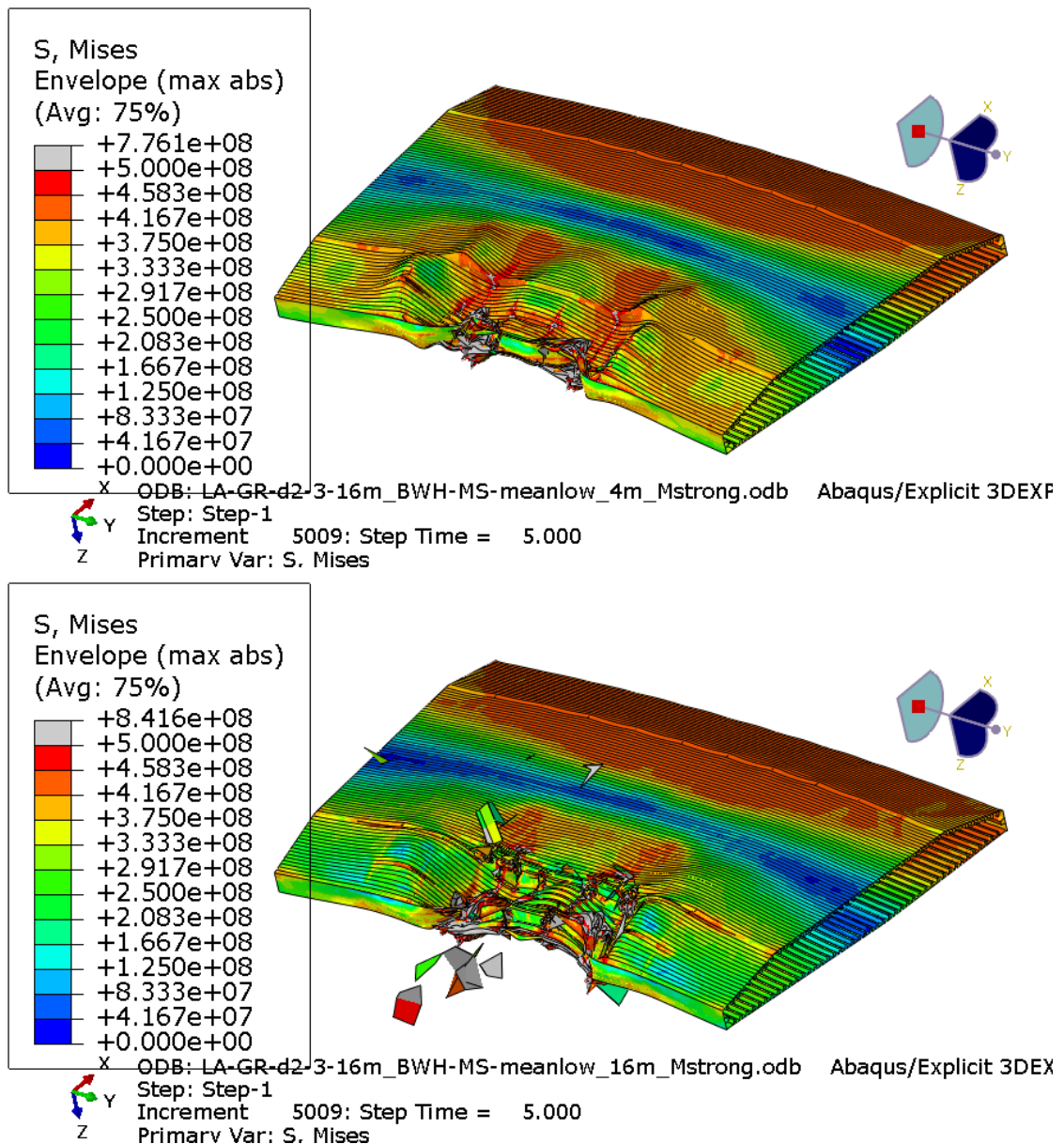
It is seen that the compression of the bridge girder to stabilize at approximately 0.8 m. Although the compression is not large, the damage is already evolved at an early stage. The risk of the necessity of repairing the bridge girder even at low impact velocities/energies is present. The design of the bridge girder side wall should perhaps be improved because of this.



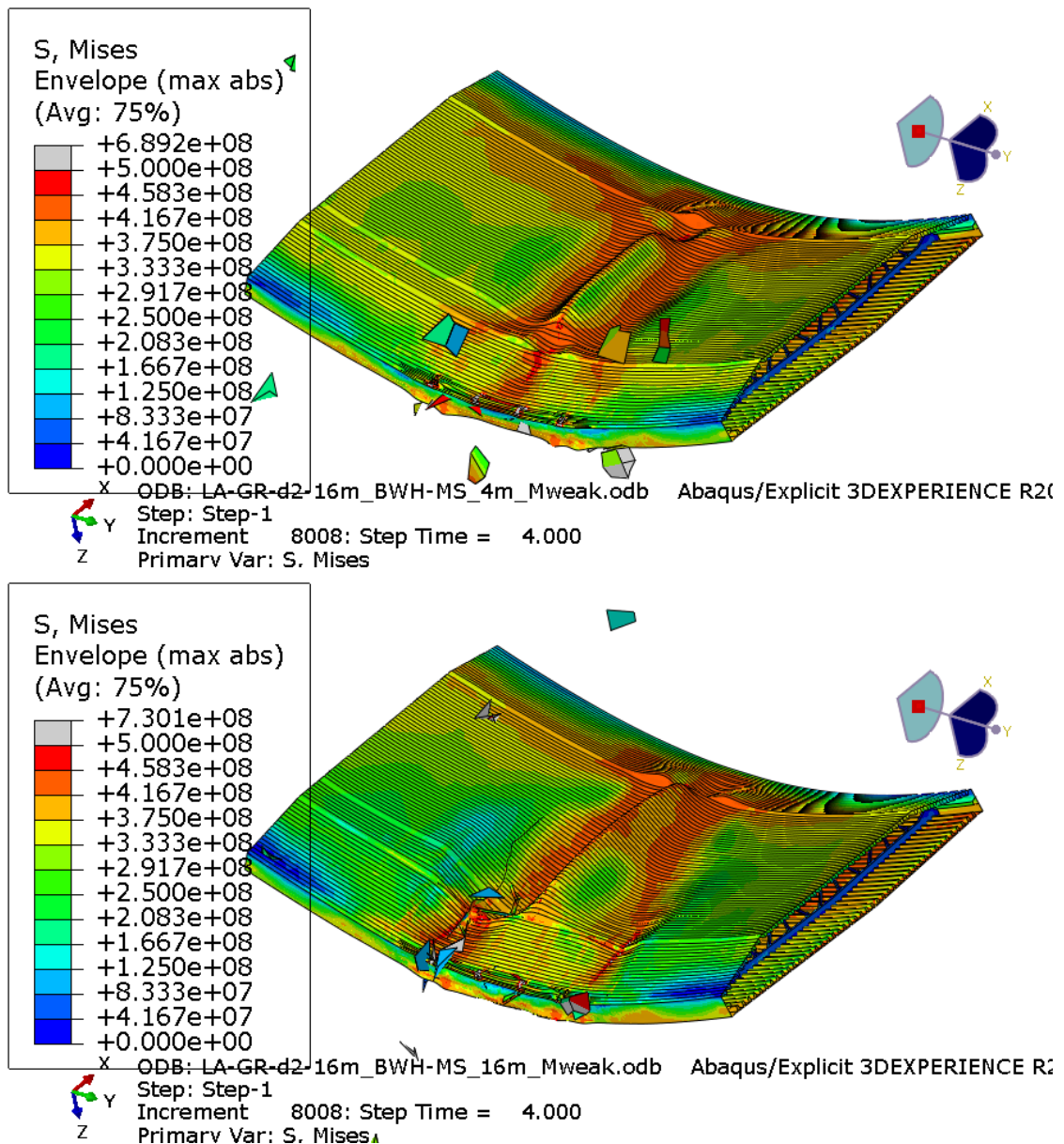
> Figure 5-9 Damaged bridge girder after approximately 4 m, 8 m, 12 m and 16 m ship displacement for impact between deck 2 and 3



> Figure 5-10 Damaged bridge girder after approximately 4 m, 8 m, 12 m and 16 m ship displacement for impact at deck 2



- > Figure 5-11 Damaged bridge girder after 4 m (upper) and 16 m ship displacement (lower) applied with moment about strong axis. Deformations are scaled with factor 10 (and cause enlargement of damaged elements).



- > Figure 5-12 Damaged bridge girder after 4 m (upper) and 16 m ship displacement (lower) applied with moment about weak axis. Deformations are scaled with factor 10 (and cause enlargement of damaged elements).

The resulting load-rotation curves are given in Figure 5-13 and Figure 5-14. The hand calculated values (without material factors) based on first yield of the girder edges are included for comparison. Table 5-3 evaluates the residual capacity as the apex of the load-rotation curves. It is seen that the reduction of capacity does not drastically fall even up to 16 m ship displacement. The reason is because the deckhouse dissipates most of the energy, while the dissipated energy in the girder almost stabilizes, see Figure 5-6. More than 16 m ship displacement is not very relevant as the deckhouse depth is 17.6 m.

The non-smooth curves and instant "jumps" seen especially in Figure 5-13 are due to explicit evaluation of the capacity. To verify this, two types of implicit analysis, dynamic implicit and Riks step, are conducted for comparison. The explicit and implicit load-rotation curves for

moment about strong axis of the intact bridge girder are shown in Figure 5-15. The explicit analysis gives higher capacity than the implicit analysis. However, for relative residual capacity evaluation the explicit solver is satisfactorily to utilize. Control of energy balance has been performed for the residual capacity models of the damaged bridge girder at 16 m ship displacement. The error is satisfactorily low for the explicit models as shown in Appendix C section 6 [22].

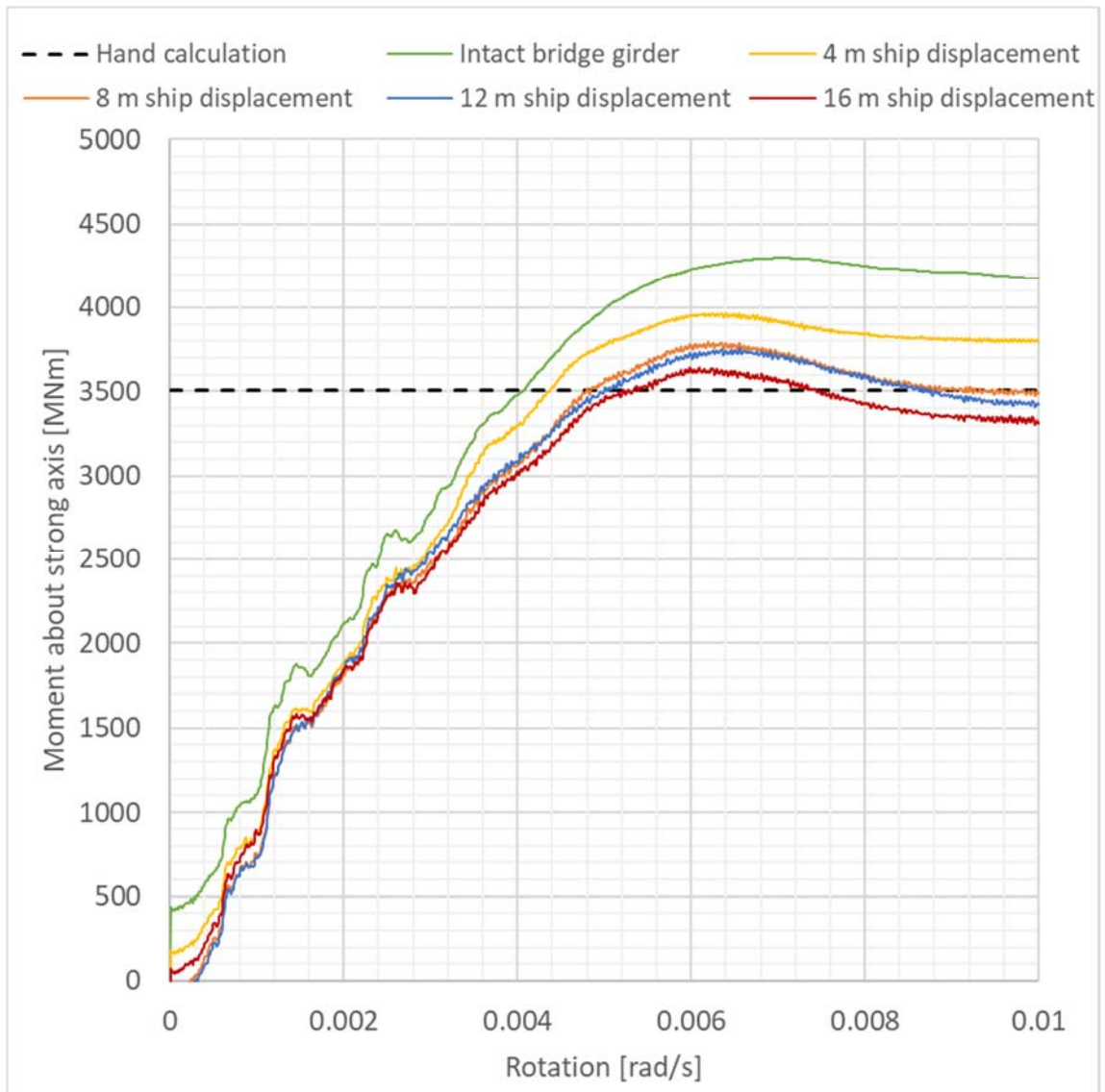


> Figure 5-13 Load-rotation curve for moment about strong axis

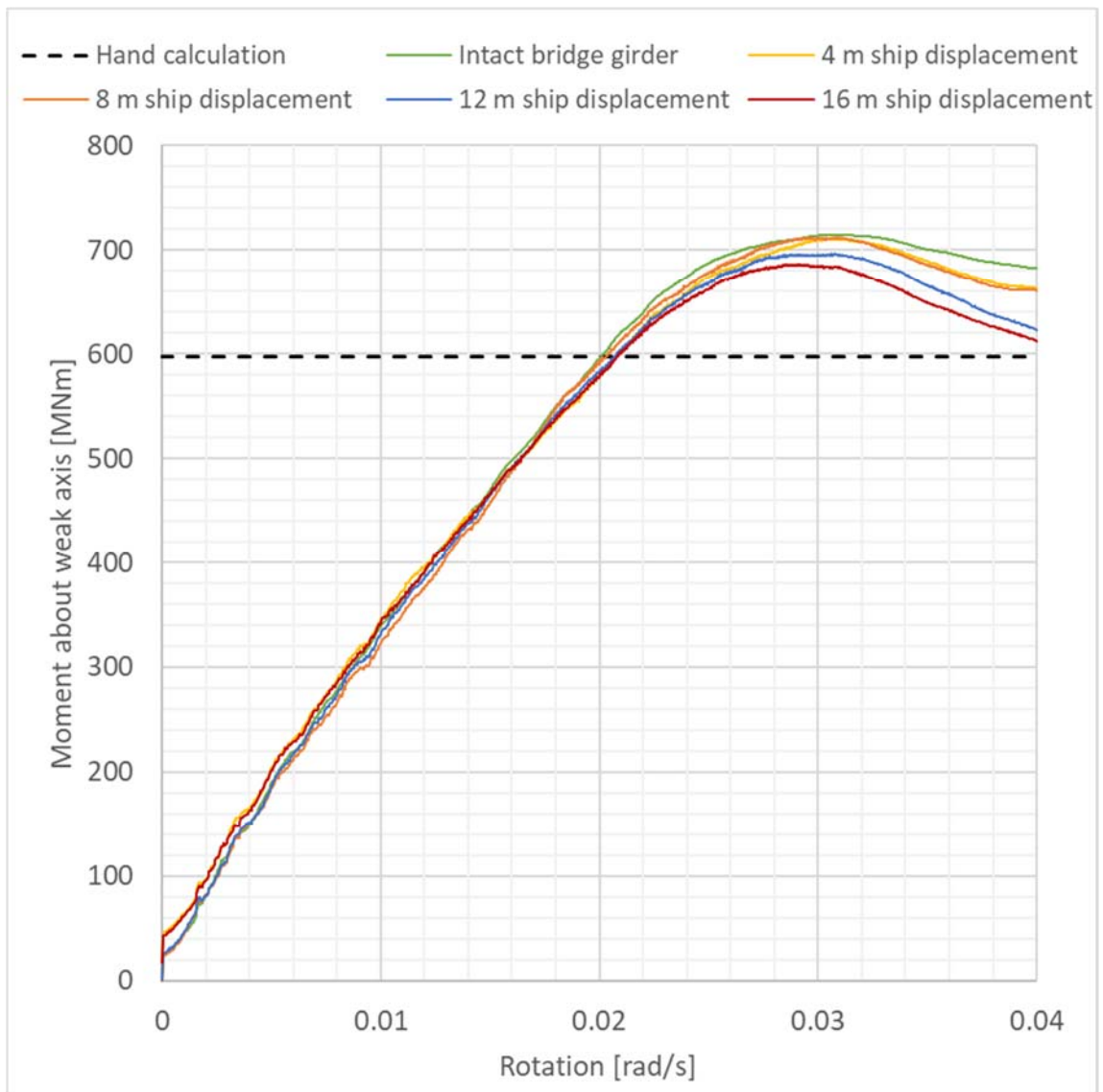


> Figure 5-14 Load-rotation curve for moment about weak axis

> Table 5-3 Residual capacity of bridge girder after ship impact

	Moment about strong axis	Moment about weak axis
Intact bridge girder	100 %	100 %
4 m ship displacement	92.3 %	99.6 %
8 m ship displacement	88.2 %	99.6 %
12 m ship displacement	87.4 %	97.4 %
16 m ship displacement	84.7 %	96.0 %

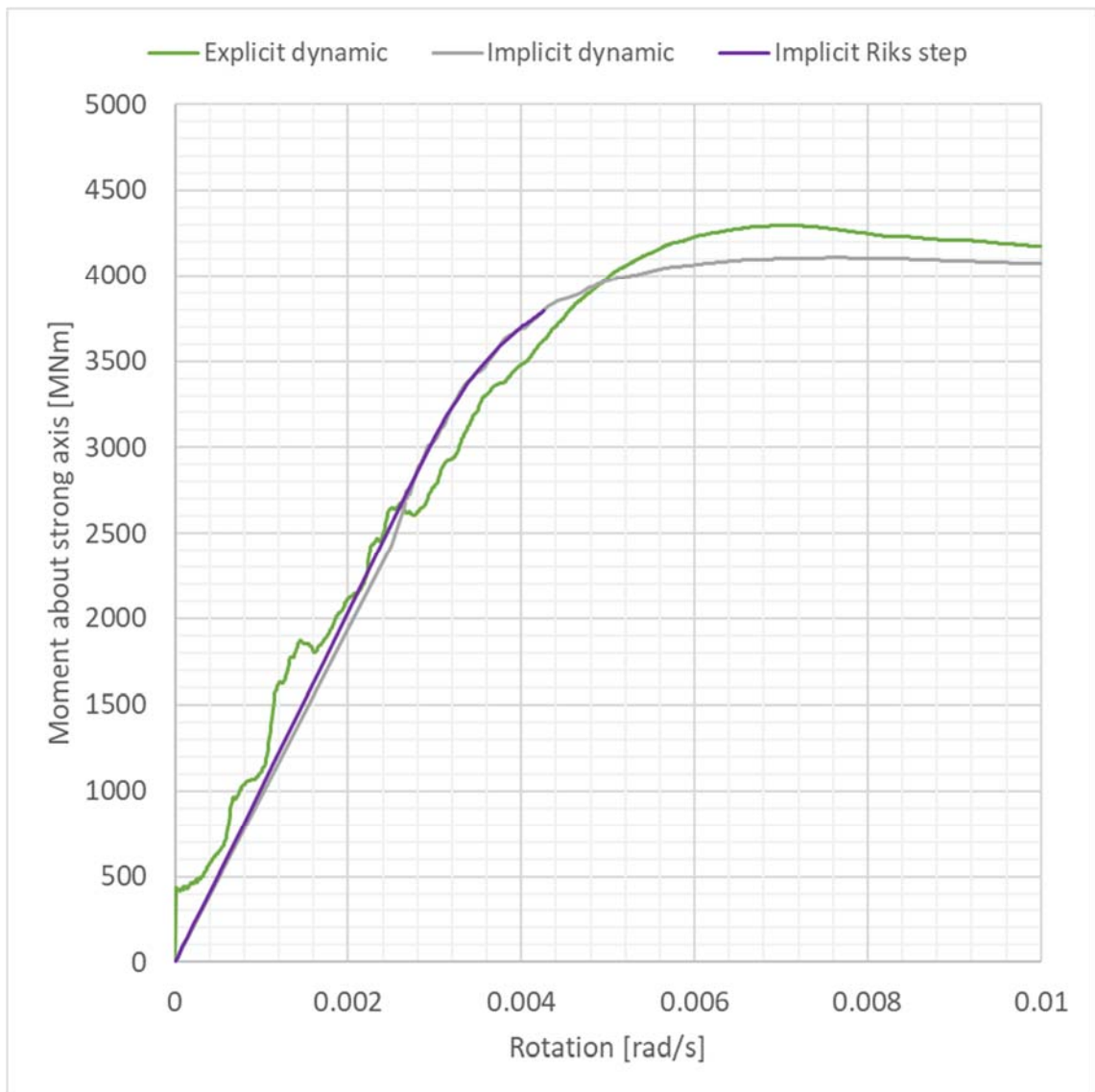


> Figure 5-15 Load-rotation curve for moment about strong axis for intact bridge girder, comparison with implicit analysis

The capacity of the bridge girder cross section can be evaluated as first yield of outer edge. For post-impact consideration with characteristic factors, the capacities of intact bridge girder are:

$$\text{Moment about strong axis:} \quad M_{z,Rd} = \frac{I_z}{y_{max}} \cdot f_y = \frac{114.926 \text{ m}^4}{13.8 \text{ m}} \cdot 420 \text{ MPa} = 3498 \text{ MNm}$$

$$\text{Moment about weak axis:} \quad M_{y,Rd} = \frac{I_y}{z_{max}} \cdot f_y = \frac{2.714 \text{ m}^4}{1.91 \text{ m}} \cdot 420 \text{ MPa} = 597 \text{ MNm}$$

The capacities of damaged bridge girder after 16 m ship displacement is evaluated with the values in Table 5-3:

$$\text{Moment about strong axis:} \quad M_{z,Rd,red} = 3498 \text{ MNm} \cdot 0.847 = 2963 \text{ MNm}$$

$$\text{Moment about weak axis:} \quad M_{y,Rd,red} = 597 \text{ MNm} \cdot 0.960 = 573 \text{ MNm}$$

Load combination 23 from the interactive result webpage [25] of K12, Model 20 gives the maximum section forces for 100-year environmental loading of cross section BCS1:

Moment about weak axis (X=5073 m): $M_{y,Ed,max} = 360 \text{ MNm} < 573 \text{ MNm} \rightarrow OK$

Moment about strong axis (X=5133 m): $M_{z,Ed,max} = 1758 \text{ MNm} < 2963 \text{ MNm} \rightarrow OK$

Note that this evaluation is very simple and does not include other section forces nor combination of section forces. Any second order effects of the global bridge structure response due to reduced stiffness at the impacted point is not accounted for. However, the utilization for the 100-year environmental loading is only about 60 % for both moments about strong and weak axis. The residual capacity of the bridge girder for the 100-year environmental loading seems satisfactory.

6 INPUT TO GLOBAL COLLISION ASSESSMENT

Global collision assessment has been performed with both “mean-low” material parameters. Impact at deck 2, load case A from Table 5-2, gives the highest impact force level. The resulting force-displacement curves are given in Figure 6-1.

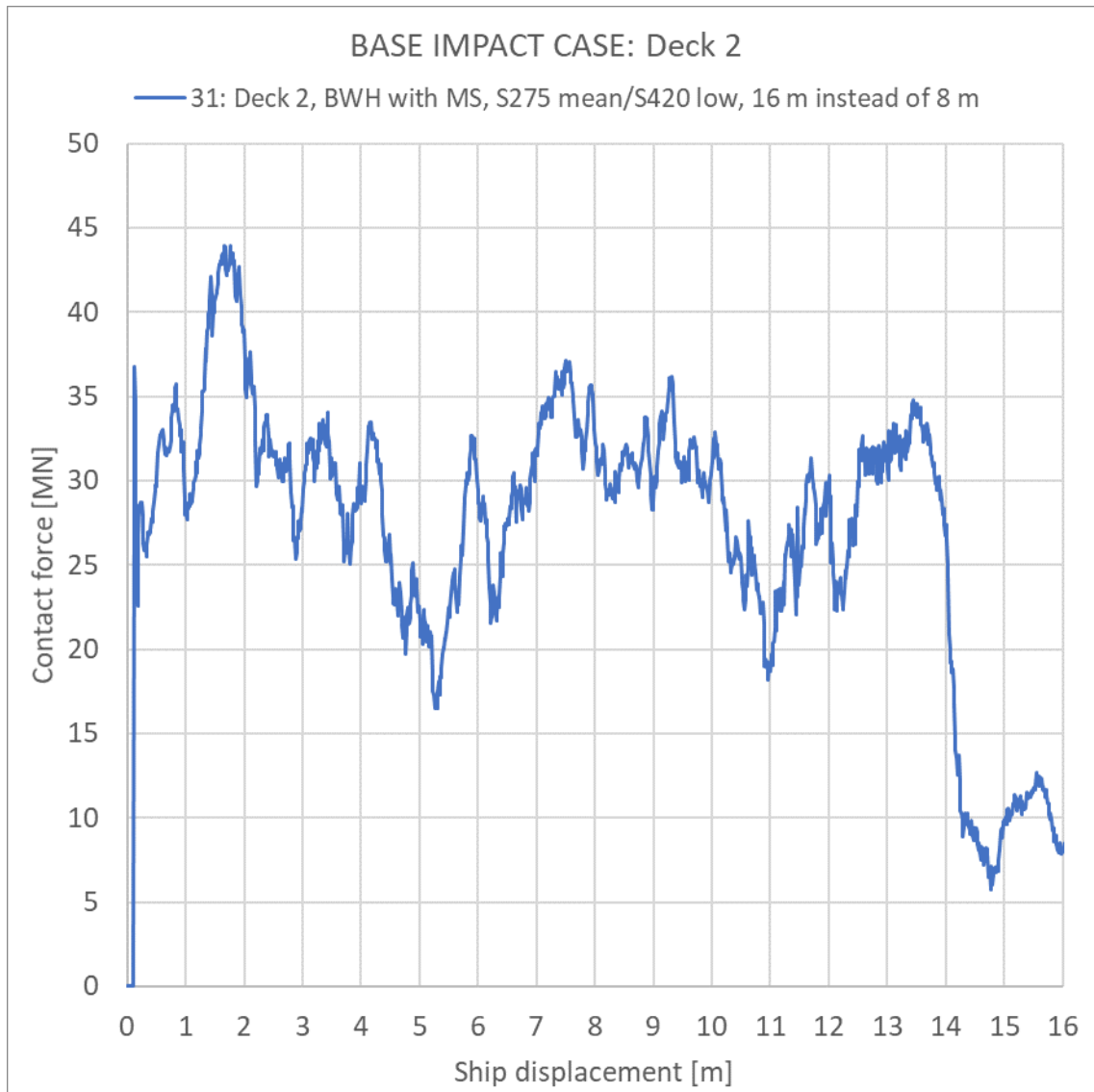


> Figure 6-1 Contact force [MN] base impact case deckhouse-girder

7 SUMMARY AND CONCLUSIONS

7.1 Compilation of response

Local response of deckhouse-girder collision with “mean-low” material parameters is considered as the most reliable simulations performed. The response of the load cases in Table 5-2 are shown in Figure 7-1 (equal to Figure 5-5).

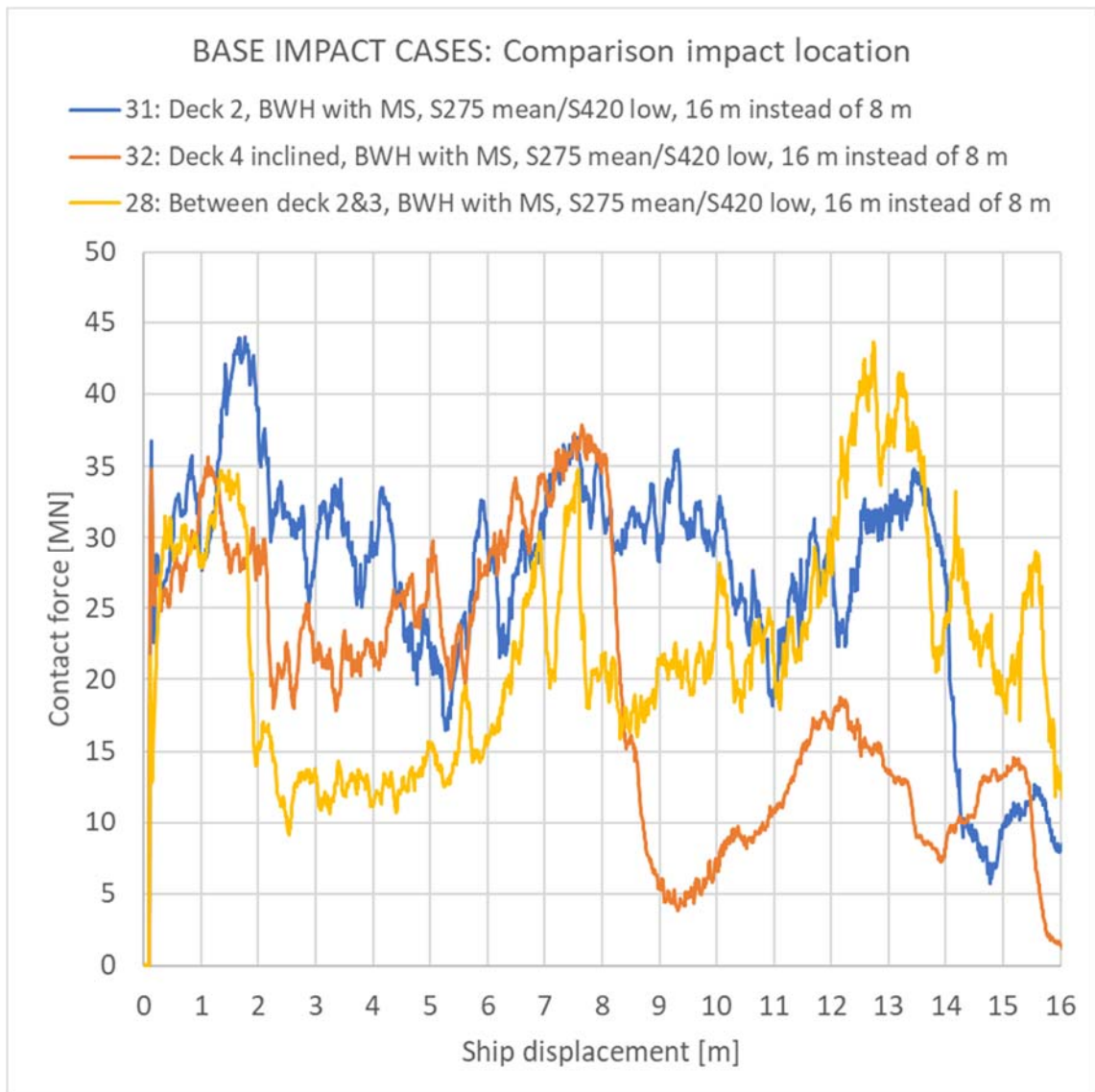


> Figure 7-1 Contact force [MN] impact deckhouse-girder

7.2 Discussion

7.2.1 Interaction with global assessment

Input from local collision response to global collision assessment is the force-displacement curves. The force-displacement curve gives the relationship between the contact force and the indentation between ship deckhouse and bridge girder. These curves are put into the global finite element model of the bridge structure by a non-linear connector element representing the ship and bridge girder locally. Details to this workflow are explained in the global assessment report [24].

When global assessment has been conducted, several response parameters are revealed for further local damage evaluation. This includes as the most important the amount of energy that is dissipated locally and the indentation between ship deckhouse and bridge girder.

In the local simulations performed, the deckhouse dissipates most of the energy while the girder is less damaged. The distribution of energy dissipation between the deckhouse and the girder is in the area 85/15 [%]. This distribution causes the compression of the bridge girder to stabilize at approximately 0.8 m, seen in Figure 5-9 and Figure 5-10. The displacement of the connector element obtained from the global assessment is therefore close to the indentation in the deckhouse alone.

When the local damage is known, reduced stiffness and capacity (reduced section modulus or second moment of inertia) and can be given as input to evaluate the damaged condition with a 100-year environmental loading applied to the bridge.

External dynamics is accounted for. Results for local impact response are therefore given for chosen parameters as basis for comparison.

7.2.2 Sensitivity of results

The ship impact simulations performed are sensitive to several parameters.

The impact force level is higher when the bridge girder hits on a deck level. If the deckhouse hits the bridge girder between two decks, the impact force is much lower. Impact low on the deckhouse is also worse because the deckhouse is stiffer close to the hull.

The following sensitivity studies are documented in Appendix C [22]:

- Material parameters defining the isotropic hardening (Appendix C section 1 [22])
- Material damage model (Appendix C section 2 [22])
- Element type (Appendix C section 3 [22])
- Mass scaling (Appendix C section 4 [22])
- Reinforced bridge girder (Appendix C section 5 [22])

The choice of material parameters defining the isotropic hardening affects the collision response. Generally, a higher material curve also represents a higher force and energy level. A low set of materials parameters is intended for design calculations. The design parameters may result in too low capacity for structures when the goal is to evaluate the impact forces. On the other hand, a high set of material parameters is considered too conservative.

Consciousness should be addressed when choosing the hardening parameters. To lower the uncertainties regarding higher material quality than accounted for, an opportunity is to

specify the maximum values to yield and ultimate tensile stress to the supplier of the bridge steel materials. Experimental test can be performed to verify the actual material quality.

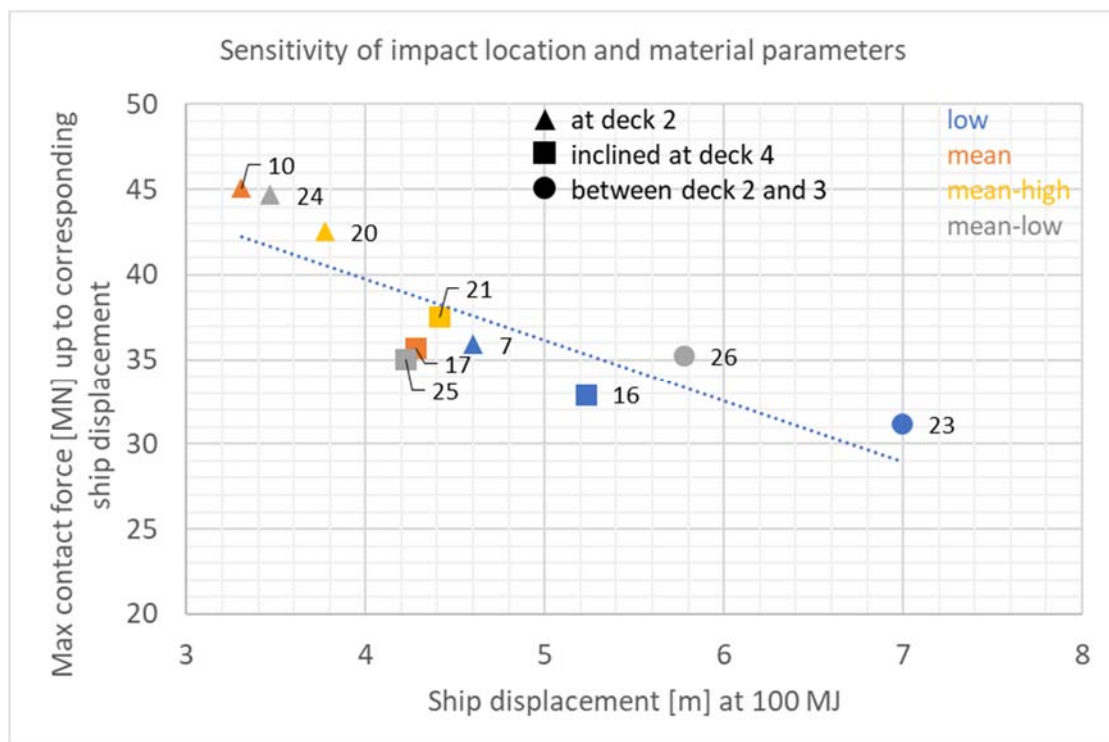
However, compared to local ship impact analysis of the pontoons [26], the bridge girder is less sensitive to material quality than the pontoons. If a mean set of material parameters is utilized for the deckhouse or other structures than can strike the bridge girder, sensitivity of material parameters for impact with the bridge girder is minimized compared to other sensitivities.

Figure 7-2 shows a graphical presentation of the sensitivity of impact location and material parameters investigated for impact with the deckhouse. The maximum contact force defined by a cut-off at ship displacement corresponding 100 MJ is plotted.

The figure shows that the simulation is sensitive to impact location. Further, the "mean-high", "mean-low" and "mean" sets of material parameters have large variation of S420 material curve, which is utilized for the bridge girder. These three set of material parameters display similar results.

The low fractile set of material parameters has low S275 material curve utilized for the deckhouse, while the other three sets of material parameters have a mean S275 material curve. The low set of material parameters gives lower maximum contact force and higher ship displacement at equal energy dissipation than the other three sets of material parameters.

This means that the simulation is less sensitive to change in material parameters of the bridge girder and sensitive to change in material parameters of the deckhouse. The reason is because the deckhouse is more damaged in collision with the bridge girder.



> Figure 7-2 Sensitivity of impact location and material parameters

Figure 7-3 shows that the local impact simulation is sensitive to the material damage models investigated. The material damage model utilized is mainly the BWH model with mesh scaling. The finite element model behaves more independently of the mesh size when mesh scaling is applied. The FLD material model display similar results to the BWH model without mesh scaling. Both these models are sensitive to coarse mesh by predicting fracture at a later state. Note that these two models predicted a bit larger damage to the girder than the BWH model with mesh scaling. This is due to the later fracture prediction of the deckhouse.

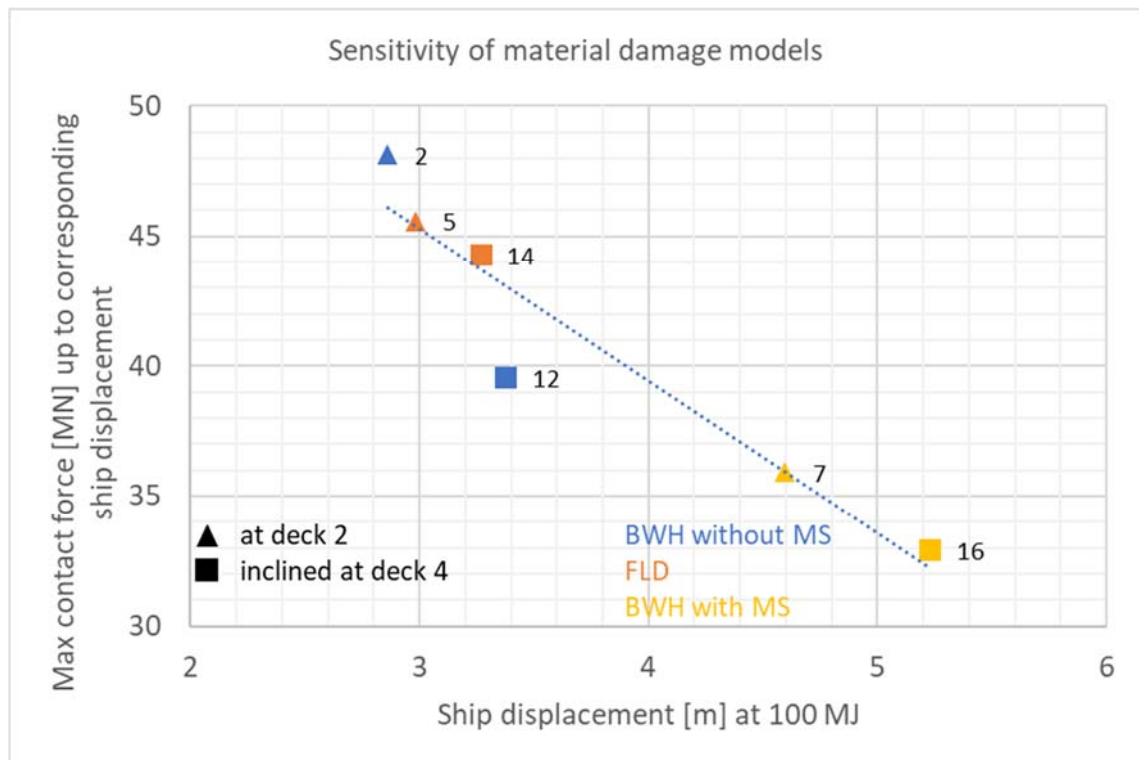


> Figure 7-3 Sensitivity of material damage models

Figure 7-4 shows the sensitivity of element type, mass scaling and reinforced bridge girder cross section investigated. The simulation is sensitive to the element type utilized in terms of reduced or full integration. Full integration displays lower force level. A higher force level is generally conservative when studying ship impact for global assessment, justifying the results with reduced integration.

Mass scaling is applied to the models to reduce computation time. This is done by applying an automatic mass scaling which limits the minimum time increment to the deckhouse, scaling 20 % of the total mass of the deckhouse-girder impact model. A simulation of deckhouse-girder collision without mass scaling has been performed. The differences were negligible, and Figure 7-4 shows that the sensitivity is low.

The sensitivity is also low for the reinforced bridge girder cross section when studying the maximum contact force for equal energy dissipation.

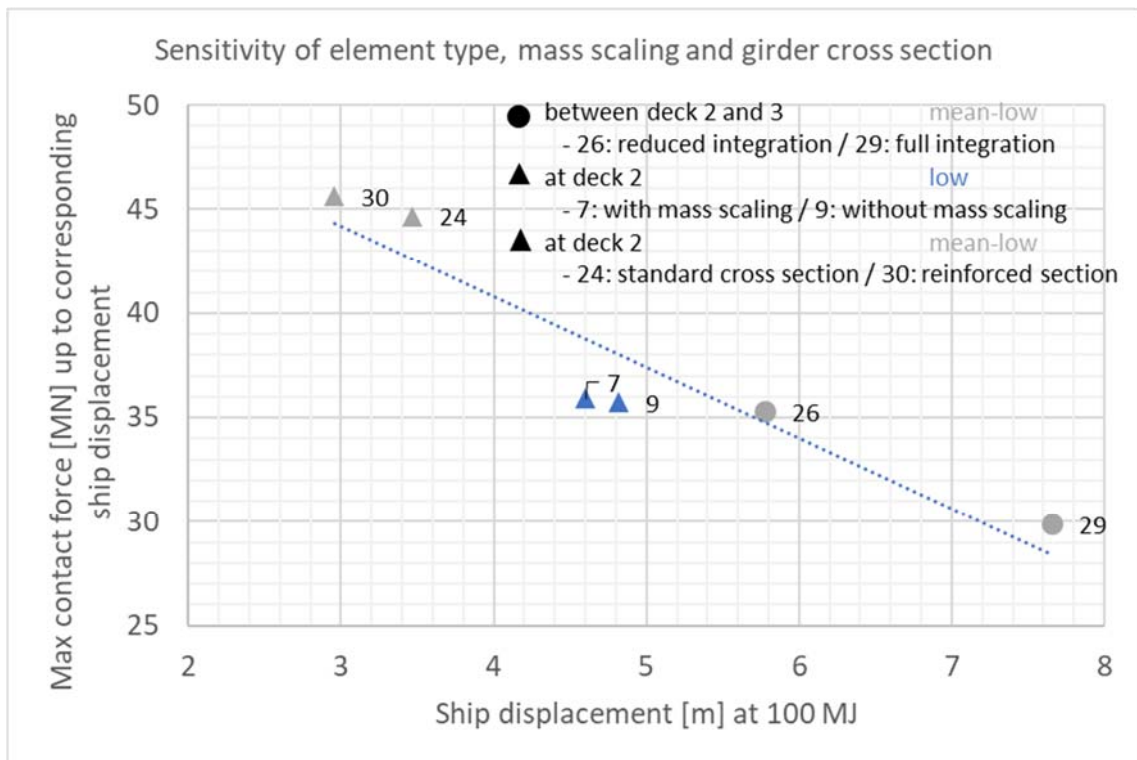


> Figure 7-4 Sensitivity of element type, mass scaling and reinforced bridge girder cross section

7.3 Further work

Further work should include updating finite element models to the final geometry of the bridge girder. Changes to ship impact design loads should be implemented. A reinforced cross section of the bridge girder should be checked to see if this results in higher impact force level.

Sensitivities to the local impact simulations can be addressed further to minimize the uncertainties. However, this is difficult if not material specification, material tests and experimental tests are performed to calibrate the local simulations. Sensitivity should be investigated for other structures that can hit the bridge girder and impact at lower velocities.

Further work related to evaluating residual capacity of the bridge girder after a ship impact should include other section forces than moment about strong and weak axis and typical load combinations of section forces. All though the documented compression of the bridge girder from ship impact is not large, the damage is already evolved at an early stage. The risk of the necessity of repairing the bridge girder even at low impact velocities/energies is present. The design of the bridge girder side wall should perhaps be improved because of this.

In the next phase, detailed design of the column-bridge girder interface must be conducted. This to make sure that the bridge's resistance against ship impact meets the requirements defined.

- [1] SBJ-32-C4-SVV-90-BA-001, "Design Basis Bjørnafjorden floating bridges," Statens Vegvesen, 2018.
- [2] SBJ-33-C5-OON-22-RE-013-B, "Concept development floating bridge E39 Bjørnafjorden - K12 - Ship impact, Global assessment," Norconsult, Dr. Techn. Olav Olsen, 2019.
- [3] Håndbok N400 , "Bruprosjektering," Statens vegvesen Vegdirektoratet, 2015.
- [4] NS-EN 1991-1-7:2006+NA:2008, "Eurocode 1: Actions on structures - Part 1-7: General actions - Accidental actions," Standard Norge, 2006.
- [5] DNVGL-RP-C204, "Design against accidental loads," DNV GL, 2017.
- [6] DNVGL-RP-C208, "Determination of structural capacity by non-linear finite element analysis methods," DNV GL, 2016.
- [7] DNVGL-OS-B101, "Metallic metals," DNV GL, 2015.
- [8] Simulia, "Abaqus/CAE 2017," Dassault Systèmes, 2016.
- [9] K. M. Ofstad, "Finite element modelling of steel bridge structures exposed to ship collisions (Matster thesis)," NTNU, Trondheim, 2018.
- [10] A. S. Hagbart, O. S. Hopperstad, R. Törnqvist and J. Amdahl, "Analytical and numerical analysis of sheet metal instability using a stress based criterion," *International Journal of Solids and Structures*, vol. 45, no. 7-8, pp. 2042-2055, 2008.
- [11] M. Storheim and J. Amdahl, "On the sensitivity to work hardening and strain-rate effects in nonlinear FEM analysis of ship collisions," *Ship and Offshore Structures*, vol. 12, no. No. 1, pp. 100-115, 2017.
- [12] Y. Sha, I. F. Osvoll and J. Amdahl, "Ship-pontoon collision analysis of the floating bridge concepts for Bjørnafjorden," NTNU, 2018.
- [13] Y. Sha and J. Amdahl, "Local deckhouse-girder collision analysis of the floating bridge concept for Bjørnafjorden," NTNU, 2018.
- [14] H. S. Alsos, J. Amdahl and O. S. Hopperstad, "On the resistance to penetration of stiffened plates, Part II: Numerical analysis," *International Journal of Impact Engineering*, vol. 36, pp. 875-887, 2009.
- [15] SBJ-20-C3-AAS-27-RE-002, "Bjørnafjorden Suspension Bridge - K1 Impact Report - Local," Aas-Jakobsen, NGI, Johs Holt, Moss Maritime, Plan Arkitekter, Cowi, Aker Solutions, 2017.
- [16] SBJ-33-C5-OON-22-RE-015-B App. B, "K12 - Ship Impact, Bridge girder, Appendix B - Mesh and material sensitivity study," Norconsult, Dr. Techn. Olav Olsen, 2019.
- [17] H. S. Alsos and J. Amdahl, "On the resistance to penetration of stiffened plates, Part I - Experiments," *International Journal of Impact Engineering*, vol. 36, pp. 799-807, 2009.
- [18] Drawing no. K7-031, "E39 Bjørnafjorden K7 End-anchored Floating Bridge," Norconsult, Dr. Techn. Olav Olsen, Aker Solutions, 2017.
- [19] Drawing no. SBJ-33-C5-OON-22-DR-142-B, "E39 Bjørnafjorden, Reksteren-Os, Concept development floating bridge, Girder, Cross-sections 1, Concept study," Norconsult, Dr. Techn. Olav Olsen, 2019.
- [20] Drawing no. SBJ-33-C5-OON-22-DR-141-B, "E39 Bjørnafjorden, Reksteren-Os, Concept development floating bridge, Girder, Cross-sections 2, Concept study," Norconsult, Dr. Techn. Olav Olsen, 2019.

- [21] M. Storheim, "Structural Response in Ship-Platform and Ship-Ice Collisions (Doctoral theses)," NTNU, Trondheim, 2016.
- [22] SBJ-33-C5-OON-22-RE-015-B App. C, "K12 - Ship Impact, Bridge girder, Appendix C - Sensitivity of ship impact response," Norconsult, Dr. Techn. Olav Olsen, 2019.
- [23] E-mail by Fredrik Lindqvist from SSAB, "Teknisk forespørsel - materialegenskaper ved stålbestilling?," Borlänge, received 2019-04-15.
- [24] SBJ-33-C5-OON-22-RE-013-B, "Concept development floating bridge E39 Bjørnafjorden - K12 - Ship impact, Global assessment," Norconsult, Dr. Techn. Olav Olsen, 2019.
- [25] Olav Olsen, Olav Olsen interactive; Project Bjørnafjorden phase 5, Oslo.
- [26] SBJ-33-C5-OON-22-RE-014-B, "Concept development floating bridge E39 Bjørnafjorden - K12 - Ship impact, pontoons and columns," Norconsult, Dr. Techn. Olav Olsen, 2019.